

# Physiological origin of biogenic magnetic nanoparticles in health and disease: from bacteria to humans

Oksana Gorobets<sup>1,2</sup>

Svitlana Gorobets<sup>1</sup>

Marceli Koralewski<sup>3</sup>

<sup>1</sup>National Technical University of Ukraine (Igor Sikorsky Kyiv Polytechnic Institute), <sup>2</sup>Institute of Magnetism, National Academy of Sciences, Kiev, Ukraine; <sup>3</sup>Faculty of Physics, Adam Mickiewicz University, Poznań, Poland

→ Video abstract



Point your SmartPhone at the code above. If you have a QR code reader the video abstract will appear. Or use:  
<http://youtu.be/81bDQkd3qil>

Correspondence: Oksana Gorobets  
National Technical University of  
Ukraine (Igor Sikorsky Kyiv Polytechnic  
Institute), 37 Peremogy Avenue,  
Kiev 03056, Ukraine  
Email pitbm@ukr.net

Marceli Koralewski  
Faculty of Physics, Adam Mickiewicz  
University, Umultowska 85, 61-614  
Poznań, Poland  
Email koral@amu.edu.pl

**Abstract:** The discovery of biogenic magnetic nanoparticles (BMNPs) in the human brain gives a strong impulse to study and understand their origin. Although knowledge of the subject is increasing continuously, much remains to be done for further development to help our society fight a number of pathologies related to BMNPs. This review provides an insight into the puzzle of the physiological origin of BMNPs in organisms of all three domains of life: prokaryotes, archaea, and eukaryotes, including humans. Predictions based on comparative genomic studies are presented along with experimental data obtained by physical methods. State-of-the-art understanding of the genetic control of biomineralization of BMNPs and their properties are discussed in detail. We present data on the differences in BMNP levels in health and disease (cancer, neurodegenerative disorders, and atherosclerosis), and discuss the existing hypotheses on the biological functions of BMNPs, with special attention paid to the role of the ferritin core and apoferritin.

**Keywords:** biogenic magnetic nanoparticles, biomineralization, ferritin, magnetoferritin, genetic control, neurodegenerative disorders, cancer

## Introduction

Living organisms have a genetically programmed ability to synthesize a wide spectrum of minerals and other inorganic substances in a process known as biomineralization.<sup>1-3</sup> Biosynthesis of so-called biogenic magnetic nanoparticles (BMNPs) from inorganic iron compounds is of particular interest, because of the magnetic properties of BMNPs.

BMNPs have been the object of intensive research since 1975, when they were first detected in magnetotactic bacteria (MTB). MTB exhibit magnetotaxis, or movement in response to a magnetic field, which makes them migrate along geomagnetic field lines.<sup>4,5</sup> In later studies, BMNPs were found in a large number of organisms of all three domains, ie, prokaryotes, archaea, and eukaryotes (Table 1).

Formed in the process of biomineralization, crystalline BMNPs are nanocrystalline forms of antiferromagnets or ferrites, such as magnetite, maghemite, or greigite (Table 2).<sup>6-9</sup> From the point of view of magnetic properties, there are two types of BMNPs, with and without remanent magnetization: those without remanent magnetization include antiferromagnetic BMNPs and ferrite BMNPs in the superparamagnetic (SPM) phase; remanent magnetization is displayed by ferrite BMNPs in single-domain (SD) and multidomain (MD) states. As a rule, ferrite BMNPs, besides being very sensitive to applied magnetic fields, are permanent nanomagnets, showing remanent magnetization in a wide temperature range (Table 2) and generating a stray

Table 1 Properties of BMNPs in different organisms

Organism	Mineral/amorphous material	Size (nm)	Shape-controlled (+), other (–)	Domain structure	Localization		References
					Intracellular (+), extracellular (–)	In chain (+), other (–)	
Magnetotactic bacteria	Magnetite and/or greigite	10–40, 35–120*	+	SD	+	+	4, 5, 9, 26, 27, 69–71
Bacteria with MSIs	Magnetite, greigite, lepidocrocite, or amorphous materials	–	–	SD, SPM	+, –	+, –	39
Archaea	Magnetite	~100*	–	SPM	+	–	39
Algae protists	Magnetite			SD			41
Worms	Magnetite	~20		SPM			35
Mollusks	Magnetite			SD			9, 72
Armored snails	Greigite			SD			42
Honeybees, butterflies, ants	Magnetite	500*–1,000*	–	SD	+	–	33, 44, 45
Termites	Magnetite	~10	–	SD, SPM		–	34
Lobster	Magnetite?			SD			46
Newts	Magnetite			SD			47
Fish	Magnetite	25–60	–	SD		+	36, 48–53, 73
Sea turtles	Magnetite?			?			54
Birds	Magnetite, maghemite	~1,000*	+, –	SPM, SD	+	+, –	38, 55, 74, 75
Bats	Magnetite?			SD			59
Dolphins, whales	Magnetite			SPM, SD, MD			60
Humans	Magnetite, maghemite hematite	<1,000	–	SPM, SD, MD	+	+	61–63, 76

Note: \*Size of BMNP clump, not single NP.

Abbreviations: BMNPs, biogenic magnetic nanoparticles; MSIs, magnet-sensitive inclusions; SD, single-domain; SPM, superparamagnetic; MD, multidomain.

**Table 2** Magnetic iron minerals found in BMNPs

Oxide	Chemical structure	Magnetic character	T <sub>c</sub> (K)	Saturation magnetization (A·m <sup>2</sup> kg <sup>-1</sup> )	References
Magnetite	Fe <sub>3</sub> O <sub>4</sub>	Ferrimagnetic	850	92–100	77
Maghemite	γ-Fe <sub>2</sub> O <sub>3</sub>	Ferrimagnetic	820	60–80, 56–74	81
Hematite	α-Fe <sub>2</sub> O <sub>3</sub>	Ferrimagnetic	956	0.3–0.4	82
Ferrihydrite	Fe <sub>5</sub> HO <sub>8</sub> ·4H <sub>2</sub> O	Antiferromagnetic	~350 <sup>a,c</sup>	0.1–1	83, 84
Wüstite	FeO	Antiferromagnetic	~203 <sup>a</sup>	–	84
Greigite	Fe <sub>3</sub> S <sub>4</sub>	Ferrimagnetic	<625	59	85
Goethite	α-FeOOH	Antiferromagnetic	400 <sup>a</sup>	0.01–1	9, 84

**Notes:** <sup>a</sup>T<sub>N</sub>, Néel temperature, which describes transition from paramagnetic to antiferromagnetic phase; <sup>b</sup>two-line, X-ray diffractometry of ferrihydrite crystals usually shows two or six lines;<sup>84</sup> <sup>c</sup>at 300 K.

**Abbreviations:** BMNPs, biogenic magnetic nanoparticles; T<sub>c</sub>, Curie temperature.

magnetic field, which in their vicinity is approximately four orders of magnitude stronger than the magnetic field of the Earth. The puzzle of the role of BMNPs in living organisms has not been solved to date, and it remains to be established whether they are involved in any biological functions other than the navigation of MTB under a geomagnetic field. Geomagnetic navigation of some migratory birds and other animals can also be explained by an alternative cryptochrome model.<sup>10</sup>

The genetic control of BMNP biomineralization has only been studied in detail in MTB, with the corresponding biomineralization proteins identified.<sup>11–15</sup> However, the physiological origin of BMNPs in other organisms, including humans, has attracted much attention for more than 30 years. The problem is very important, since elevated BMNP levels are associated with a number of human diseases, including neurodegenerative disorders and cancer.<sup>16–21</sup> Until recently, there had been only one hypothesis: that ferrihydrite present in the ferritin core might be a precursor of biogenic magnetite. Indeed, ferrihydrite has been proved experimentally to be a transient mineral in the formation of magnetite in cells of MTB<sup>22</sup> and in chiton teeth.<sup>9</sup> Still, ferritin has not been found experimentally to participate in biomineralization of BMNPs. Another hypothesis on the physiological origin of BMNPs in prokaryotes, archaea, and eukaryotes, including humans, recently predicted by bioinformatic methods, postulates a common genetic mechanism of BMNP biomineralization based on homologues of biomineralization proteins of MTB.<sup>23</sup> In this review, we outline experimental and theoretical investigations of the role of biomineralization proteins, especially ferritin, in the physiological origin of BMNPs, and we point out the importance of environmental pollution only as another source of MNPs in the human body. Our intention is to aid in better understanding of the cellular production of BMNPs for efficient treatment of a number

of diseases representing an urgent problem that our society is facing now and will face in the future. In the following sections, we discuss the physicochemical properties of BMNPs, the genetic control of BMNP biomineralization, the physicochemical characteristics of natural and synthetic ferritin, and the question of whether the ferritin core is a precursor of BMNPs.

## Physicochemical properties of BMNPs

### BMNPs in MTB magnetosomes

MTB synthesize NPs of magnetic crystals enclosed in a membrane, a structure known as a magnetosome vesicle. Single-crystal magnetite or greigite is incorporated in the magnetosome membrane, which besides phospholipids contains a number of magnetosome-associated proteins (Figure 1A).<sup>12,24,25</sup> Magnetosomes in MTB are arranged in chains,<sup>4–6</sup> bearing dozens of separate magnetite NPs of size 10–135 nm<sup>26,27</sup> (see Figure 1B and C). These BMNP chains follow the long axis of the bacterium, and are attached to its membrane.<sup>11</sup> The NPs in a chain may have different crystal geometries, including octahedral, cubic, hexagonal prismatic, bullet, teardrop, and arrowhead morphologies (see examples in Figure 1D).<sup>28–30</sup> BMNPs are not the byproduct in MTB, but the process of biomineralization of BMNPs is energy-consuming.<sup>31</sup>

### BMNPs in bacteria, archaea, and multicellular organisms

BMNPs have been observed in many prokaryotes, archaea, and eukaryotes (Figure 2, Table 1).<sup>4–7,9,32–40</sup> However, as already mentioned, for the first time BMNPs have been revealed in MTB that are characterized by the ability to “taxi” or navigate under a geomagnetic field. That is why historically the idea of magnetotaxis was transformed into an

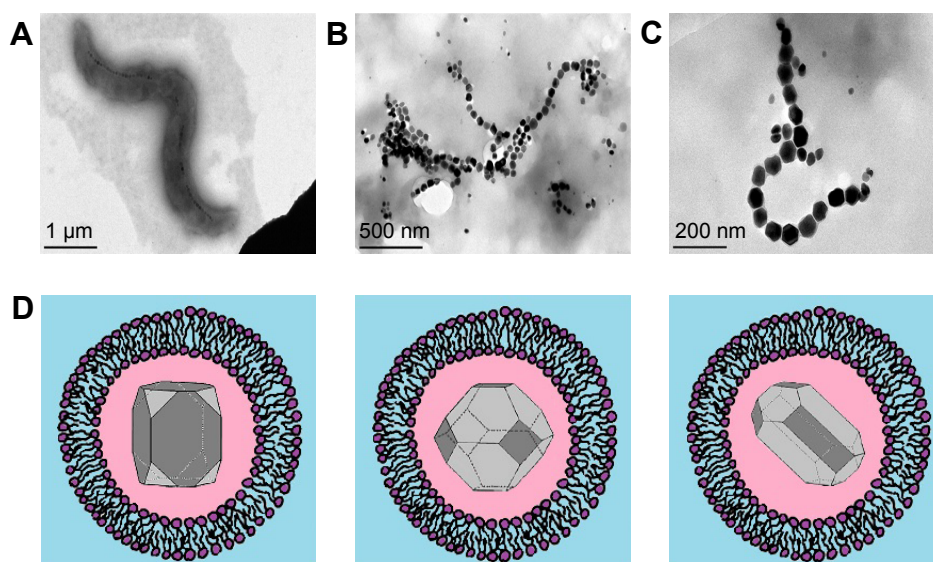


**Figure 1** (A) TEM of magnetotactic bacterium (*Magnetospirillum* strain AMB1); (B) BMNP chain in a magnetotactic bacterium; (C) zoomed BMNP chain, showing several hexagonal grains (TEM courtesy of B Leszczyński); (D) schematic representation of BMNPs in a magnetosome vesicle. BMNPs of typical shapes observed in magnetotactic bacteria, each surrounded by lipid bilayers.

**Abbreviations:** TEM, transmission electron microscopy; BMNP, biogenic magnetic nanoparticle.

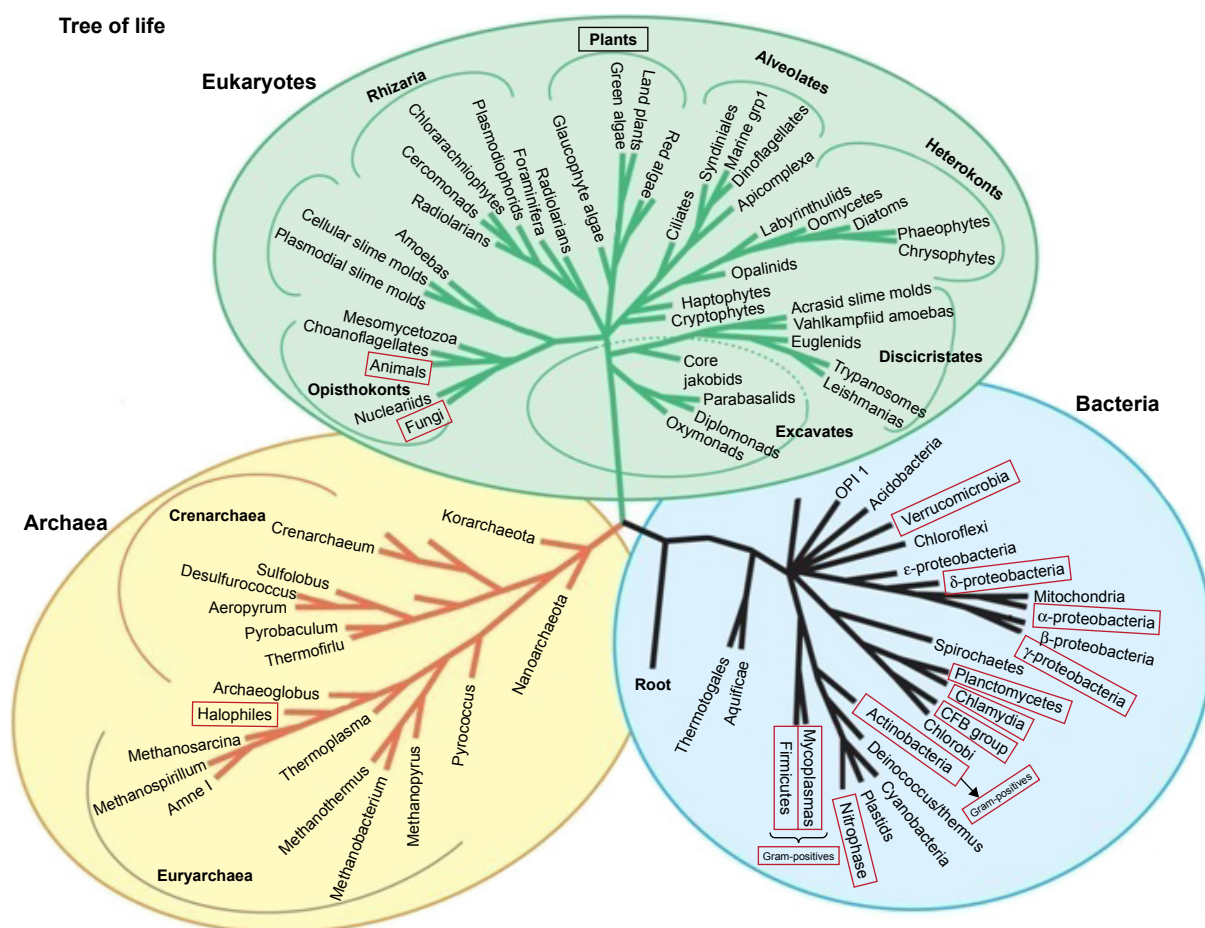


**Figure 2** Taxa in which BMNPs have been observed experimentally.

**Notes:** Red boxes, BMNPs found in representatives of the given taxa; black rectangle, reported presence of biogenic magnetite in an unclear form (either phytoferritin or botanic BMNPs).

**Abbreviation:** BMNPs, biogenic magnetic nanoparticles.



idea of magnetoreception as a basic function of BMNPs in other organisms. However, many bacteria with BMNPs<sup>39</sup> are immovable, and some multicellular organisms with BMNPs are not able to migrate long distances.<sup>35</sup> Consequently, the question about the physiological origin of BMNPs and properties of BMNPs in organisms should be considered from a broader aspect, independently of their ability to navigate Earth's magnetic field.

More specifically, BMNPs have been found experimentally in algae, protists,<sup>41</sup> worms,<sup>35</sup> chitons,<sup>37</sup> armored snails,<sup>42</sup> ants, butterflies,<sup>43–45</sup> honeybees,<sup>33,44</sup> termites,<sup>34</sup> lobster,<sup>46</sup> newts,<sup>47</sup> fish,<sup>36,48–53</sup> sea turtles,<sup>54</sup> birds,<sup>38,55–58</sup> bats,<sup>59</sup> dolphins, whales,<sup>60</sup> and humans.<sup>8,16,17,22,61–67</sup> Table 1 provides general information on BMNPs in different organisms.

The phenotypic manifestation of BMNPs in multicellular organisms, archaea, and non-MTB differs in many ways from that of BMNPs in MTB. As a rule, BMNPs in multicellular organisms vary in shape, size, and other properties, and are not enclosed in magnetosome vesicles.<sup>39,68</sup> In archaea, in which the surroundings of BMNPs have been adequately investigated, magnet-sensitive inclusions have been found, which are surrounded by a homogeneous matrix with organic (mainly protein) components.<sup>39</sup> The absence of vesicles or a similar organic matrix consisting of protein filaments around magnetite BMNPs<sup>68</sup> has also been observed in human cells. In multicellular organisms, most BMNPs display remnant magnetization and are SD structures. However, MD and/or SPM phases have also been observed in some multicellular organisms (Tables 1 and 2).

In magnetite, transition from the SPM to SD phase typically occurs in the size range 25–30 nm,<sup>77</sup> and transition from SD to MD around 70 nm.<sup>78</sup> Magnetostatic interactions between magnetite NPs reduce the SPM-to-SD transition size in chains of SD grains; at the same time, the SD-to-MD transition size increases as a result of this interaction, which significantly extends the size range of the SD phase.<sup>78</sup> This is due to magnetostatic interaction fields wherein the largest magnetosome crystals observed in living bacteria (250 nm long with an aspect ratio of 0.84)<sup>79</sup> have an SD structure;<sup>80</sup> without magnetostatic interaction, they would be in an MD state.

## BMNPs in normal human organs and tissues

BMNPs have been found in various human organs, including heart, liver, spleen,<sup>64,86,87</sup> adrenal glands,<sup>65</sup> ethmoid bone,<sup>88</sup> and brain.<sup>8,20,61,89,90</sup> In terms of phenotypic manifestation, human BMNPs differ in many ways from those observed in MTB. Separate single-crystal BMNPs and BMNP clumps of rather irregular shape have been observed in human tissues.

Clumps are arranged in long chains<sup>61,91</sup> associated with the membrane. A chain is several micrometers long and comprises up to 80 NPs.<sup>61</sup> Magnetite clumps in tissues are aggregates of single-crystal particles that have remnant magnetization at 150 K. This excludes magnetic contribution from ferritin (which is superantiferromagnetic and behaves as a paramagnet at this temperature), diamagnetic bulk tissue, and paramagnetic (PM) ions.<sup>19</sup> Unlike MTB, human BMNPs have a wide size range and are observed in all phases of growth. Consequently, SPM and SD phases coexist,<sup>8</sup> and human BMNPs vary in shape, size, and other properties. Also, the number of BMNPs in normal human tissues varies widely. For example, the number of MNPs per gram of tissue in pia and dura ranges from 5 million to 100 million.<sup>61</sup>

In summary, there are similarities between the production of BMNPs in humans and MTB production of magnetite NPs, organized in chains (see Figures 1, 3, and 4) of dozens of NPs, attached to the cell membrane. There are also different features of BMNPs in MTB and humans. BMNPs in humans are not characterized by control of morphology or size and are not surrounded by lipid magnetosome vesicles.

## BMNPs in human disease

The problem of the physiological origin of BMNPs gains in importance in light of the discovery of BMNPs in a number of human organs and tissues<sup>61,91</sup> and their observed relation to neurodegenerative disorders,<sup>16,17,19,67</sup> cancer (Figure 3),<sup>20,21</sup> and atherosclerosis (Figure 4).<sup>92</sup> Concentrations of BMNPs in inflammation zones in neurodegenerative diseases<sup>93–97</sup> and cancer<sup>8,20</sup> are higher than those observed in normal tissues.

Therefore, normal iron homeostasis is disrupted in the brain in many neurodegenerative diseases.<sup>20</sup> BMNPs (magnetite and maghemite) are detected in senile plaques and tau filaments in brain tissue affected by neurological and neurodegenerative diseases, such as epilepsy and Alzheimer's disease (AD).<sup>19,66,98</sup> Concentrations of magnetite are significantly higher in samples of AD tissue than in healthy tissue.<sup>19</sup> The total concentration of biogenic magnetite is 15 times greater in the AD brain than controls in some cases.<sup>16</sup> Magnetite NPs are present in amyloid- $\beta$  (A $\beta$ ) plaque cores, and are directly bound into fibrillar A $\beta$ .<sup>99</sup> Magnetite NPs have been found to be directly associated with AD plaques and tangles.<sup>66,89,99,100</sup> In vitro experimental data show that magnetite enhances the toxicity of A $\beta$ .<sup>101</sup>

BMNPs have been detected in various human tumor tissues, including melanoma, breast, ovary, testicle, sarcoma, meningioma, glioblastoma, astrocytoma, glioma, and metastasis.<sup>20</sup> An elevated quantity of BMNPs is observed in tumor samples in comparison with normal ones. For example,

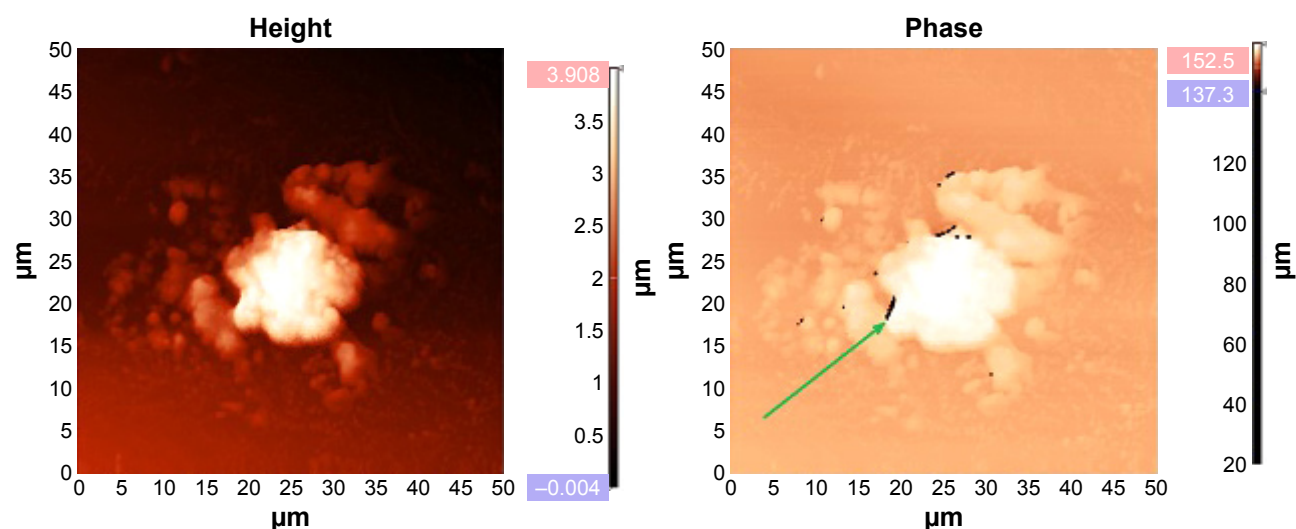


**Figure 3** Ehrlich carcinoma cell.

**Notes:** AFM (left), MFM (right). Data from Chekchun et al.<sup>21</sup> MFM shows BMNPs in the form of dark spots arranged in chains (arrow).

**Abbreviations:** AFM, atomic force microscopy; MFM, magnetic force microscopy; BMNPs, biogenic magnetic nanoparticles.

human meningioma brain-tumor tissues contain approximately ten times the concentration of BMNPs of nontumor hippocampus.<sup>8</sup>

Magnetic force microscopy (MFM) reveals BMNPs arranged in chains of various lengths up to several microns long (see the MFM images in Figures 3 and 4). Both biogenic and anthropogenic origins of MNPs are found in human tissues.<sup>102,103</sup> The presence of BMNPs can lead to increased accumulation of MNPs, due to magnetic dipole–dipole interaction between biogenic and anthropogenic MNPs. This is

important in connection with the influence of polluted urban environments on human health.<sup>102</sup>

## Genetic control of biomineralization of BMNPs

Detection of elevated levels of BMNPs in disease raises questions. Is elevated BMNP production the cause or consequence of disease? What genes are controlling this process in humans? In perspective, the answers to these questions would result in new methods of treatment and diagnostics

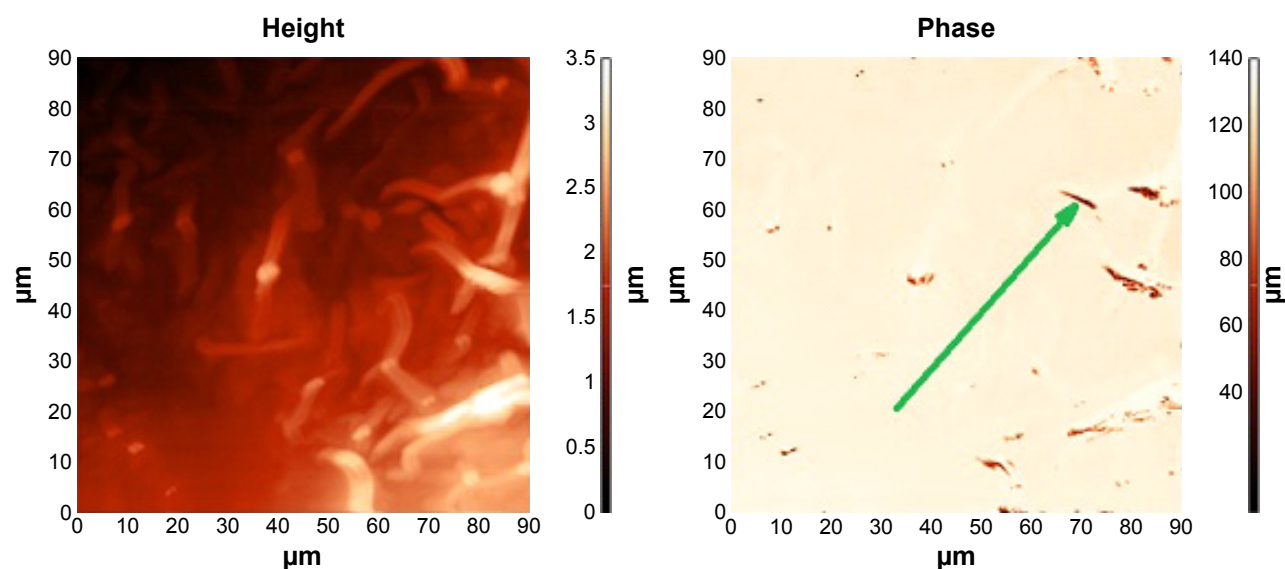


**Figure 4** Fragment of an atherosclerotic plaque of mixed composition.

**Notes:** AFM (left), MFM (right). MFM shows BMNPs in the form of dark spots arranged in chains (arrow). There were no bacteria-like magnetosome BMNPs, but alignment of the BMNPs is visible along the plaque surface. Samples of atherosclerotic vessels were extracted from iliac artery during shunting surgery.

**Abbreviations:** AFM, atomic force microscopy; MFM, magnetic force microscopy; BMNPs, biogenic magnetic nanoparticles.

of cancer, atherosclerosis, and neurodegenerative disorders, with application of advances in genetic therapy and more sensitive specialized analytical methods. Besides, revealing the genetic mechanisms of biomineralization of BMNPs in bacteria would allow the spread of applications of bacteria with natural ferrimagnetic properties as vectors for magnetic field-assisted drug delivery systems,<sup>104</sup> including non-MTB.<sup>105</sup> For example, recent achievements have demonstrated experimental transfection of human mesenchymal stem cells with the *MMS6* gene of *Magnetospirillum magneticum* AMB1 and bioassimilated synthesis of intracytoplasmic MNPs by mammalian cells.<sup>106</sup>

## Biom mineralization proteins of MTB

To date, genetic control of the synthesis of BMNPs has only been studied experimentally in MTB,<sup>11–15</sup> where it appears to be strictly regulated by the properties and structural organization of the BMNPs.<sup>11,12</sup> Most of the magnetosome-associated proteins are encoded in the magnetosome island, in MamGFDC, Mms, and MamAB operons.<sup>107</sup> Also, the shape and size of mature magnetite NPs (Figure 1), precisely defined for each strain of MTB, are a manifestation of genes of the magnetosome island.<sup>11,29,30,108</sup>

There are two functional classes of proteins of the MTB magnetosome island (Table 3): proteins indispensable for the process of biomineralization of BMNPs, and other proteins, including regulatory proteins, which exercise strict genetic control of size distribution, species-specific morphologies, and localization of single-crystal magnetite NPs in the cell of a magnetotactic bacterium and proteins with unknown functions or of no effect on BMNP biomineralization.<sup>1,11,12</sup> The loss of the magnetosome island leads to a nonmagnetic phenotype of MTB demonstrating its key role in the biogenesis of BMNPs.<sup>11,97,109–113</sup> Figure 5 shows the participation of proteins of a magnetosome island in the biomineralization of BMNPs in a magnetotactic bacterium. The magnetosome vesicle represents a unique pool providing favorable chemical surroundings for magnetite crystal growth. Black

hexagonal symbols represent BMNP crystal growth inside magnetosome vesicles (Figure 5). The magnetosome membrane contains the magnetosome-associated Mam and Mms proteins of the magnetosome island (Figure 5).

The protein MamA (which is known also as Mms24 or Mam22) takes part in the activation of BMNP biomineralization and formation of magnetosome vesicles.<sup>26,110</sup> The proteins MamB and MamM are transporters of Fe<sup>2+</sup> and other cations, such as Co<sup>2+</sup>, Zn<sup>2+</sup>, and Cd<sup>2+</sup>. The proteins MamB and MamM take part in the formation of BMNP crystals.<sup>11,107,109–113</sup> It has been proved that mutant MTB lacking MamA, MamE, MamO, MamB, MamM, or MamN proteins can form only empty magnetosome vesicles without BMNPs.<sup>11,107,109–113</sup> That is why these proteins are indispensable for the process of biomineralization of BMNPs in MTB. The proteins MamK and MamJ take part in the formation of linear chains of BMNPs.<sup>11,107,109–114</sup> Proteins indispensable for the process of biomineralization of BMNPs have been studied,<sup>26,199,110</sup> and also regulatory proteins of the magnetosome island.<sup>107,109,111,112</sup> Figure 5 depicts the biomineralization of BMNPs in MTB and specifies the localization of biomineralization proteins.

## Human homologues of MTB proteins involved in BMNP biomineralization

Comparative genomic studies have been carried out in search of common ways of genetic regulation of BMNP biomineralization in both prokaryotes and eukaryotes, including humans.<sup>23,115</sup> Sequence alignment of human proteins with the magnetosome-island proteins of bacteria *M. gryphiswaldense* have shown significant similarities with proteins indispensable for magnetite biomineralization.<sup>23</sup> Of the 17 regulatory proteins of the magnetosome island, only one, MamK, responsible for the formation of BMNP chains, has a human homologue.<sup>23</sup> This is consistent with the phenotypic manifestations of BMNPs in MTB and in humans. Chains of BMNPs have been observed experimentally in human tissues in MFM studies (Figures 3 and 4).

**Table 3** Functional classes of proteins encoded by genes in the magnetosome island<sup>26,30,107,109–113</sup>

Functions of proteins in biomineralization of BMNPs	Proteins of the magnetosome island	References
Proteins indispensable for biomineralization of BMNPs	MamB, MamM, MamA, MamE, MamO, MamN	11, 107, 109–113
<b>Regulatory proteins responsible for</b>		11, 107, 109–113
• vesicle formation	MamQ, MamL	11, 107, 109–113
• magnetosome-chain formation	MamJ, MamK	11, 107, 109–113
• quantity, shape and size of Fe <sub>3</sub> O <sub>4</sub> particles	MamF, MamD, MamT, MamP, MamR, MamS, Mms6	30, 11
Proteins with unknown functions or of no effect on BMNP biomineralization	MamH, MamX, MamY, MamZ, MamC, MamG	11, 113

**Abbreviation:** BMNPs, biogenic magnetic nanoparticles.



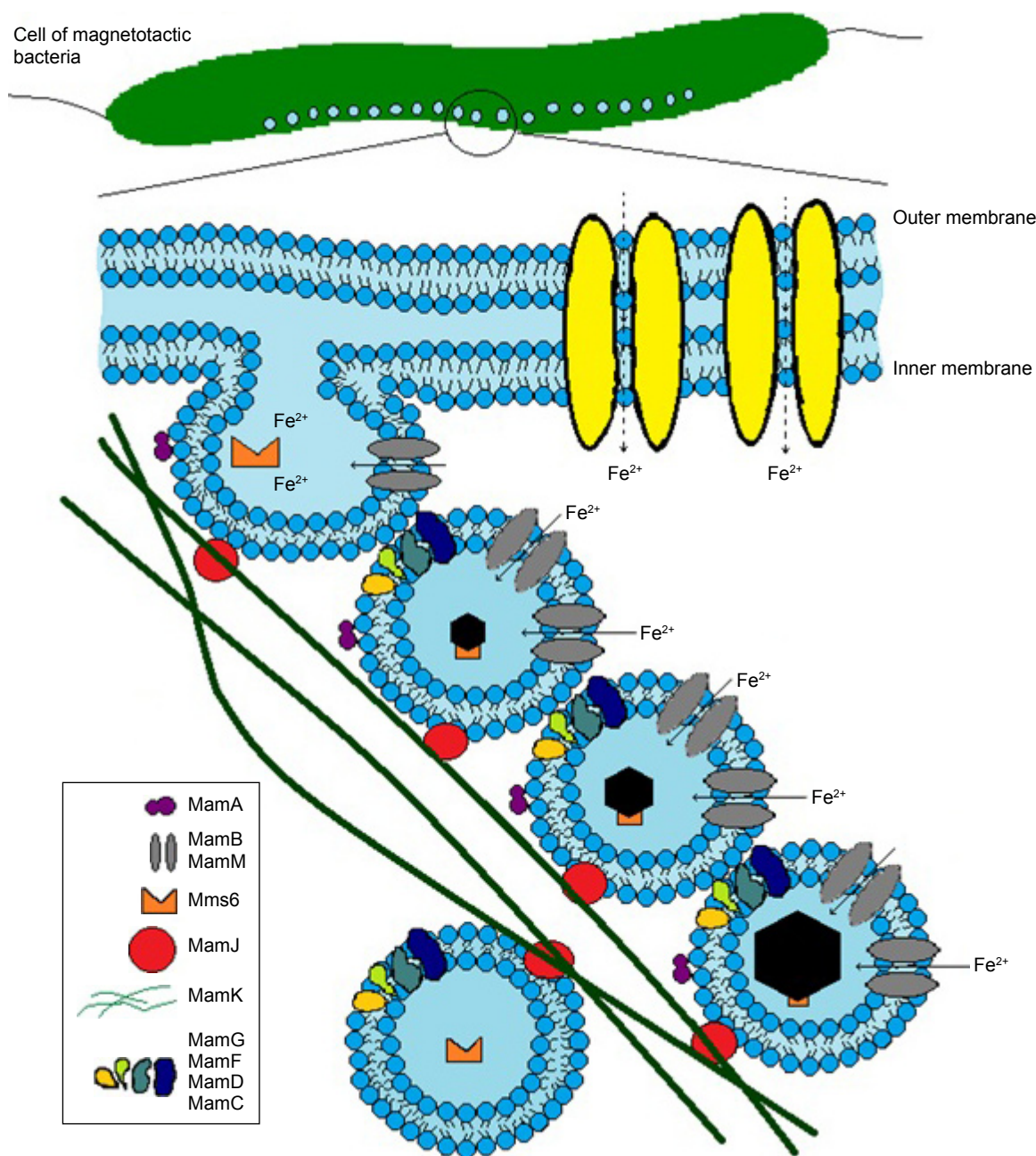


**Figure 5** Schematic representation of BMNP biomineralization in magnetotactic bacteria.

**Note:** Black hexagonal symbols represent magnetic crystal growth inside magnetosome vesicles.

**Abbreviation:** BMNP, biogenic magnetic nanoparticle.

The absence of human homologues of the other regulatory proteins of the magnetosome island in MTB is in agreement with experimental data,<sup>20,61</sup> indicating the lack of control of the size, form, and quantity of BMNPs and the absence of magnetosome vesicles in human cells.

A common genetic mechanism of BMNP biomineralization, shared by organisms of all three domains of life and based on homologues of MTB proteins indispensable for BMNP biomineralization, has been predicted by comparative

genomic methods (Tables 4 and 5).<sup>23,115</sup> Human homologues of MTB proteins indispensable for biomineralization of BMNPs are specified in Table 4. Table 5 provides a functional comparison between MTB proteins indispensable for BMNP biomineralization and their human homologues, based on National Center for Biotechnology Information (NCBI) functional annotation. The Mam proteins and their human homologues are found to have the same known functions and domains.



**Table 4** Statistically significant alignment of MTB proteins with human proteins based on BLAST standard parameters<sup>23</sup>

MTB protein	MamA	MamB	MamM	MamN	MamE	MamO
Human	PEX5	ZnT9	ZnT9	Permease P	HtrA1	HtrA1
homologue	proteins	ZnT10	ZnT4		HtrA2	HtrA2
					HtrA3	
					HtrA4	

**Abbreviations:** MTB, magnetotactic bacteria; BLAST, Basic Local Alignment Search Tool.

## Predicted common genetic mechanism of BMNP biomineralization in prokaryotes, archaea, and eukaryotes

Bioinformatic methods allow comparison of a query protein with a specific set of proteins from a database by sequence alignment of amino acid residues. Statistically significant alignments or matches among the sequences compared are used for finding homologues, ie, proteins descending from a common ancestor. Homologues of proteins necessary for BMNP biomineralization in MTB have been found in nonmagnetotactic organisms with intracellular BMNPs by sequence alignment of Mam proteins with proteins from the NCBI database.<sup>116</sup> This has provided the basis for a prediction of the biomineralization of intracellular BMNPs in eukaryotes, nonmagnetotactic prokaryotes, and archaea. Figure 6 depicts such a prediction with indicated homologues of MTB proteins indispensable for BMNP biomineralization.

It is predicted<sup>23,115</sup> that homologues of indispensable biomineralization proteins of magnetosome islands have analogous functions in control of biomineralization of BMNPs in nonmagnetotactic organisms, including humans (Figure 6, Tables 4 and 5). There is no lipid magnetosome vesicle surrounding BMNPs<sup>68</sup> or homologues of proteins responsible for vesicle formation in humans.<sup>23,115</sup> That is why it is possible that the favorable chemical surroundings for BMNP growth are provided inside the organic matrix or another type of organic material (Figure 6), as is observed in non-MTB with BMNPs.<sup>39</sup>

Not all nonmagnetotactic organisms have a homologue of the MamK protein.<sup>116</sup> This is consistent with the experimental observation of BMNPs not arranged in chains.<sup>39</sup> However, BMNP chains can form even without MamK. Biogenic and artificial magnetite NPs can arrange in chains also as a result of magnetic dipole–dipole interaction (Figure 7).<sup>117,118</sup> Aggregation of BMNPs, based on magnetic forces alone, can allow the formation of less orderly aggregate assemblies from archaea to human cell systems.

## The mineral core of ferritin: a precursor of BMNPs?

A protein that supplies iron in cells,<sup>119–121</sup> ferritin has been considered a possible precursor of BMNPs since 1996.<sup>22,122,123</sup> A hypothesis has been proposed that the ferrihydrite core of ferritin can be a precursor of magnetite, by analogy to what is observed in MTB, which in an early growth stage produce

**Table 5** Comparative table of functions of MTB proteins and their human homologues<sup>23,116</sup>

MTB protein	MTB-protein functions	Name and functions of human homologue
MamB	Cation (Co <sup>2+</sup> , Zn <sup>2+</sup> , Cd <sup>2+</sup> , Fe <sup>2+</sup> ) transporter	ZnT9, ZnT10: Zn-cation transporters; changes in these proteins in brain regions are associated with Alzheimer's disease (AD); disturbance of zinc homeostasis plays a role in the pathogenesis of AD
MamE	Serine protease; the PDZ domain of this trypsin-like serine protease is involved in response to heat shock, chaperone function and apoptosis, and may be responsible for substrate recognition and/or binding	HtrA serine proteases, involved in important physiological processes including regulation of mitochondrial homeostasis, apoptosis and transmission of cell signals involved in the development of pathological processes such as cancer and neurodegenerative diseases, including AD
MamA	TPR domain-containing protein; based around a defined consensus sequence and identified in a variety of organisms, including bacteria, cyanobacteria, yeast, and fungi, TPR domains are involved in a variety of functions, which include protein-protein interactions, chaperone functions, the cell cycle, transcription, and protein transport	Pex5: peroxisome receptor, a TPR domain-containing protein; peroxisome is a widespread cell organelle surrounded by a membrane with a large variety of metabolic functions, such as destruction of toxic compounds and construction of the myelin sheath of nerve fibers
MamN	Permease P: the exact function of this protein is unknown, but it is believed to be involved in pH adjustment, together with the ATP-driven proton pump	Human permease P: the exact function of this protein is unknown, but it is believed to be involved in pH adjustment, together with the ATP-driven proton pump
MamO	Serine protease	HtrA2 serine protease
MamM	Cation (Co <sup>2+</sup> , Zn <sup>2+</sup> , Cd <sup>2+</sup> ) transporter	ZnT4, ZnT9: Zn-cation transporters

**Abbreviations:** MTB, magnetotactic bacteria; TPR, tetratricopeptide repeat.

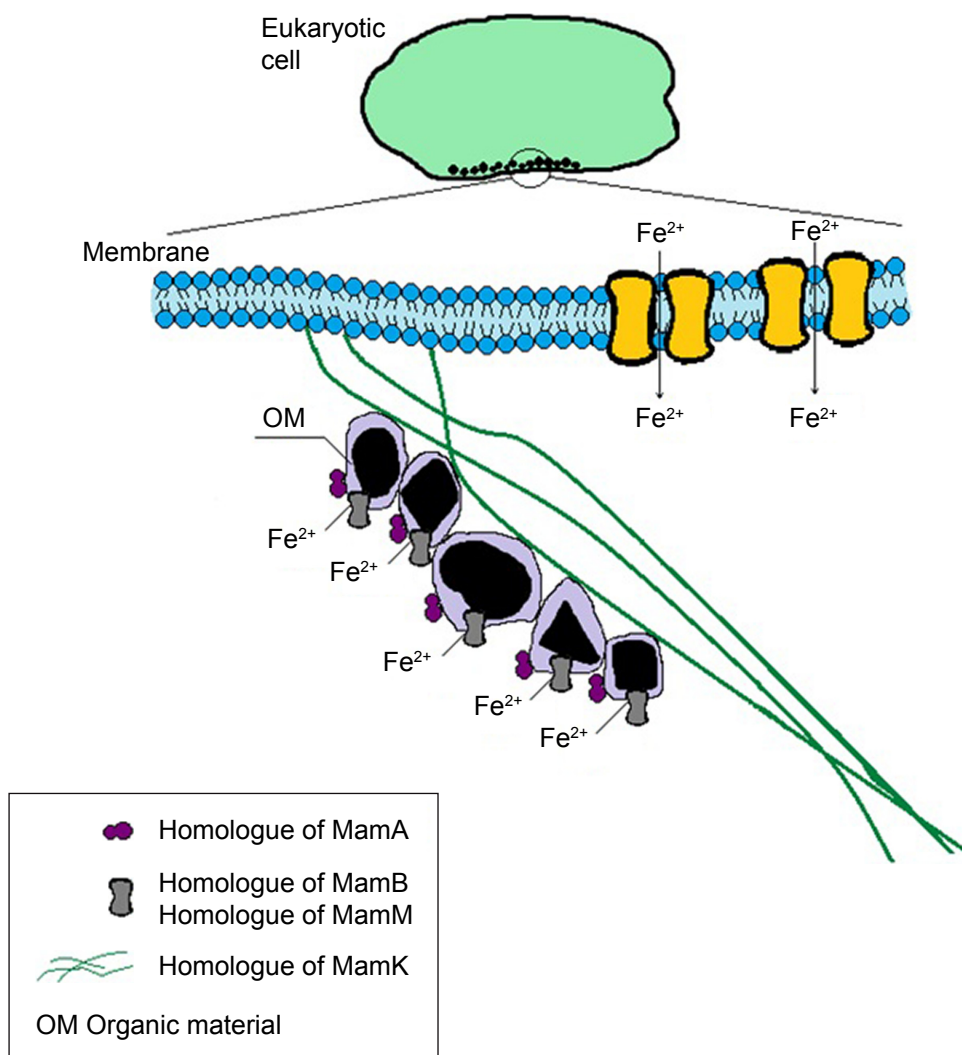


**Figure 6** Predicted biomineralization of intracellular BMNPs in eukaryotes, nonmagnetotactic prokaryotes, and archaea.

**Note:** Black shapes represent the magnetic crystals inside some organic material.

**Abbreviation:** BMNPs, biogenic magnetic nanoparticles.

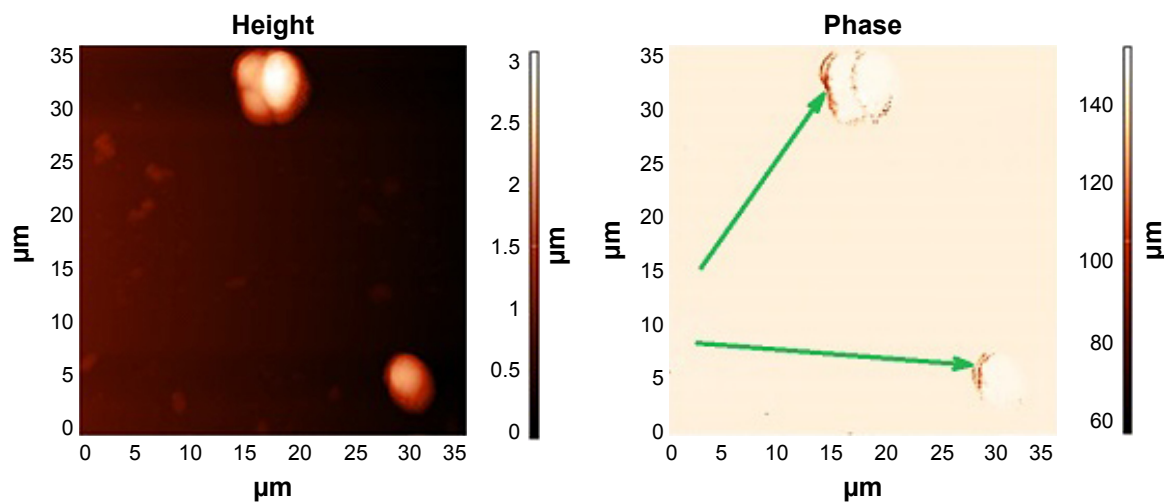


**Figure 7** *Saccharomyces cerevisiae* yeast cells with magnetic nanoparticles.

**Note:** AFM (left) and MFM image (right), showing chains (arrow) of artificial magnetic nanoparticles formed at the biomembranes of the cells, due to magnetic dipole–dipole interaction among the magnetic nanoparticles.

**Abbreviations:** AFM, atomic force microscopy; MFM, magnetic force microscopy.

noncrystalline ferrihydrite, later converted to magnetite, within the magnetosome vesicle.<sup>22</sup> However, the relation between ferritin and BMNPs seems indirect, involving the protein shell rather than the mineral core of ferritin, as indicated by its role in neurodegeneration, associated with the presence of MNPs in the human brain.<sup>122,124</sup> Though long considered,<sup>22</sup> whether the ferritin molecule is the precursor of BMNPs in human tissues has not been established to date. Also, the role of ferritin in the physiological origin of BMNPs from the point of view of the predicted common genetic mechanism of BMNP biomineralization,<sup>23</sup> as well as the interaction between ferritin and the basic set of proteins indispensable for BMNP biomineralization, remains an open question.

## Basic physicochemical characterization of ferritin

Iron is an element of vital importance to nearly all living organisms. At the same time, it is highly toxic in excess. Free  $\text{Fe}^{2+}$  ions are known to produce highly reactive oxygen species that may cause cell damage. Organisms have developed a way of fast scavenging of excess iron ions by storing them in a safe mineral form inside ferritin molecules. Discovered by Laufberger in 1937,<sup>125</sup> ferritin has been found since in most living organisms, from microorganisms to plants, invertebrates, and vertebrates, particularly mammals. Covering a broad spectrum of its properties and applications, the literature on ferritin is voluminous. We refer the reader to classical<sup>126,127</sup> and recent review papers<sup>128,129</sup> discussing the most important aspects of its physicochemical properties. Herein, we only outline these briefly, along with the methods used for studying the magnetic properties of ferritin.

### Ferritins

Ferritin is a hollow spherical protein made up of 24 subunits; iron ions are sequestered in its cavity. The iron core of the protein is described as a mineral with a form similar to that of ferrihydrite, with a stoichiometry of  $[\text{FeO}(\text{OH})]_8$

$[\text{FeO}(\text{H}_2\text{PO}_4)]$  and different amounts of phosphate.<sup>126,128,129</sup> The empty ferritin shell is known as apoferritin. The protein with iron in the cavity is referred to as holoferritin, or very often simply ferritin.

For decades ferritins, have been considered synonymous with the function of iron storage. The ferritin family includes subfamilies of mammalian, plant, and bacterial ferritins, each composed of 24 subunits. However, in recent years it has become clear that there are also other proteins able to store iron in the form of a mineral core in their central cavity. These include Dps, a subfamily of proteins made up of 12 subunits, often referred to as miniferritins. Another subfamily of protein cages, frataxin is composed of up to 48 subunits. In Table 6, we provide the main information on proteins belonging to the ferritin family. It is worthy of note that the Fe:P ratio varies considerably in native ferritin cores. The Fe:P ratio has an influence on the core morphology; however, no general rules have been observed to date.

The ferritin nanocage has a 432-point symmetry with three fourfold, four threefold and six twofold axes<sup>126,129</sup> (see Figure 8). Dps family members have only 32-point symmetry. The maximal number of iron ions that can be stored in the ferritin cavity is 4,500 (500 in Dps). The actual number of iron ions in natural ferritin depends on the organism and the organ in which it is stored. There are two types of monomers among the 24 subunits that constitute the ferritin molecule: the heavy (~21 kDa) subunit, or H-chain, comprising 178 amino acids, and the light (~19 kDa) subunit, or L-chain, of 171 amino acids.

Only one type of subunit, with a mass of 26.5 kDa, has been identified in the plant ferritin phytoferritin.<sup>131</sup> However, some authors distinguish its three forms with different molecular weight.<sup>131</sup> Some bacteria have a heme group incorporated in their ferritin, which in that case is referred to as bacterioferritin.

The H-chain carries a ferroxidase center, which appears to be essential for iron incorporation, whereas the L-chain

**Table 6** Properties of proteins of the ferritin family

Protein	Symmetry	Number of subunits	Outer/inner diameter (nm)	Iron content, atoms	References
Human ferritin	432	24	7–8/12	Up to 4,500	126, 129
Animal ferritin	432	24	8/12	Up to 4,500	128, 130
Bacterial ferritin	432	24	8/12.5	~1,600	128
Bacterioferritin	432	24	8/12.5	Up to 2,700	128
(contains heme)					
Phytoferritin	432	24		~2,000	131
(plant ferritin)					
Dps	23	12	5/9	500	132
Frataxin	?	48	?	~2,400	133

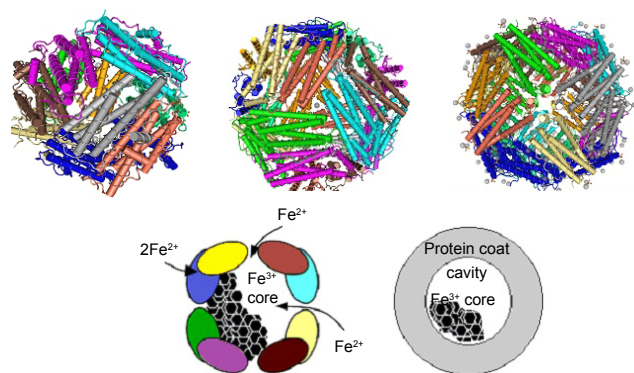


**Figure 8** Schematic representation of ferritin molecule with twofold-, threefold-, and fourfold-symmetry axes.

**Notes:** Dps, PDB – 4DYU (top left); structure of human ferritin L-chain, PDB – 2FG8 (top center); structure of human ferritin L-chain, PDB – 2FFX (top right) (NCBI). The protein-shell diameter is 12 nm, and the core diameter 7–8 nm (right).

**Abbreviations:** PDB, Protein Data Bank; NCBI, National Center for Biotechnology Information.

facilitates iron mineralization within the cavity. Plant and bacterial ferritins have only a single type of subunit, which probably fulfills both functions. Vertebrate ferritins are heteropolymers that assemble in specific H:L ratios and vary widely with organism and tissue.<sup>126,129</sup> The most often studied – horse-spleen ferritin (HSF) – is composed of ~10% of H-chains and ~90% of L-chains. Ferritins rich in L-chains predominate in iron-storage organs, such as spleen and liver, whereas heart cells and a majority of brain cells tend to contain mostly H-chain-rich ferritins. Apparently, the H:L ratio plays an important role in controlling iron concentration in

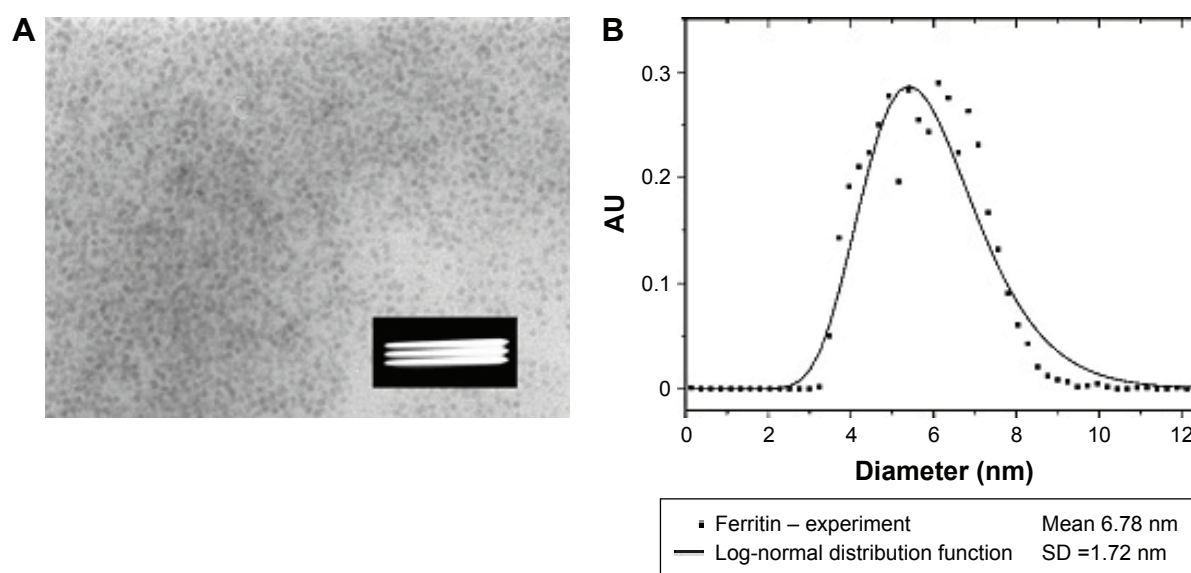
cells; this has not been fully elucidated to date, but may be related to several pathologies observed in humans.<sup>124,134</sup>

Figure 9A shows transmission electron microscopy (TEM) of well-defined NP crystallites, ie, the core of ferritin of size 3.5–8 nm within holoferritin. The particle-size distribution of ferritin, but also of any MNPs, is very often described by known distribution functions.<sup>135</sup> The log-normal distribution function is the most commonly used,<sup>136</sup> and allows the calculation of average diameter of the particle and standard deviation (Figure 9B).

The ferritin core is antiferromagnetic<sup>137</sup> with a Néel temperature of 240–460 K, but not uniquely determined.<sup>138</sup> The magnetization of the core is about two orders of magnitude lower than that of magnetite<sup>84</sup> (see Table 2). The magnetic moment of ferritin ranges from 100  $\mu_B$  to 300  $\mu_B$ , while the magnetic moment of magnetite of similar dimensions is of the order of  $10^4 \mu_B$ .<sup>139</sup> The superantiferromagnetism of ferritin NPs has been investigated recently by a combination of low-field susceptibility and magnetization measurements, and full-saturation magnetization has proved unattainable even in a magnetic field as high as 55 T.<sup>140,141</sup>

HSF tends to be regarded as a model system, and has been studied by several techniques, specified in Table 7. However, the physicochemical properties of human isoferritins have not been sufficiently studied to date, and require further investigations and correlation with human health data.

Today, ferritin is a powerful clinical tool,<sup>121</sup> but the magnetic structure of its core has not yet been explored by clinicians. It is noteworthy that a number of currently



**Figure 9** (A) Ferritin TEM (HSF), the white stripes inside the black box indicate the scale bar 100 nm; (B) particle-size distribution based on TEM.

**Abbreviations:** TEM, transmission electron microscopy; HSF, horse-spleen ferritin; SD, standard deviation.



**Table 7** Methods for study of magnetic properties of biogenic and synthetic ferritin and BMNPs

Method	Properties studied	Resolution	References
Mössbauer spectroscopy	Fe valence	≈0.2 nm	142–145
SQUID magnetometry	Magnetization	~10 nm	19, 146
Transmission electron microscopy	Electron density, phase, and periodicity	≈50 pm	61, 62, 147, 148
Nuclear magnetic resonance	Molecule structure, dynamics, reaction state, and chemical environment	50–100 nm	149
Magnetic force microscopy	Magnetic interactions	10–30 nm	21, 92, 150, 151
X-ray absorption near-edge structure	Valence, interatomic distances, and bond angles	0.1–0.5 nm	152, 153
Small-angle X-ray scattering	Shape, size, characteristic distances of partially ordered materials, pore size	5–25 nm	154, 155
Magneto-optical spectroscopy	Type of mineral	2–30 nm	139, 156–160
Electron energy-loss spectroscopy	Interatomic distances and coordination	~0.1 nm	154
Electron paramagnetic resonance	Valence		161, 162

**Abbreviations:** BMNPs, biogenic magnetic nanoparticles; SQUID, superconducting quantum-interference device.

available techniques allow the study of the magnetic properties of the core of ferritin of any origin. These include X-ray absorption near-edge structure (XANES) spectroscopy, Mössbauer spectroscopy, MFM, and magneto-optical spectroscopy (see Table 7).

Some of the methods specified in Table 7 can have clinical analytical applications. Magneto-optical spectroscopy seems a very good candidate, as it is not too sophisticated, relatively inexpensive, and can be used for studying liquid and thin-tissue samples. It is important to note that recently a rapid detection method for malaria diagnosis based on a magneto-optical method (Cotton–Mouton effect) was presented and tested.<sup>163,164</sup> Magneto-optical relaxation methods are successfully used in controlling the functionalization of magnetic particles through measurements of size of prepared molecules.<sup>165</sup>

Elevated ferritin levels are associated with inflammatory conditions, including malignancy.<sup>166</sup> In plasma, which normally contains mostly L-chain-rich ferritin, increased concentrations of H-chain-rich ferritin are observed in some pathological conditions.<sup>167</sup> Also, pathological ferritin is observed in a number of human diseases.<sup>133,168,169</sup> The interest in the chemical composition of both physiological and pathological ferritin is stimulated also by the hypothesis that the magnetic core of ferritin and aggregates of pathological ferritin might be a precursor of BMNPs.<sup>62</sup> A large number of papers have been aimed at verification of the idea that biogenic magnetite in humans might originate from ferritin, and the determination of the role of ferritin and BMNPs in the pathogenesis of diseases.<sup>100,122,124,169,170</sup> We would like to point out the environmental pollution by radiofrequency electromagnetic fields used in mobile telephony throughout the world and the long-term exposure of those who use mobile phones. There are very few papers devoted to the

possible biological effects of this radiofrequency field studied at the molecular level, though the problem has at least been discussed by Céspedes et al.<sup>171,172</sup> They found that exposure of about 2 hours to a magnetic field of 30 μT at 1 MHz on ferritin have reduced their iron intake rate by about 20%.

## Hemosiderin

The literature devoted to hemosiderin is strongly correlated with ferritin; however few studies on hemosiderin alone have been undertaken,<sup>100,173–177</sup> although it is thought that hemosiderin may play an important role directly or indirectly in iron cytotoxicity and thus deserves more intensive study. The hemosiderin aggregates found in diseases might play a similar role as ferritin doses as precursors of BMNPs; however, no direct evidence for this is known.

Water-insoluble tissue iron deposits are known as hemosiderin. Hemosiderin is thought to be a breakdown product of ferritin, and is much less soluble than ferritin. In several iron-overload diseases (eg, thalassemia or hemochromatosis) iron oxyhydroxide particles are mostly found in the form of insoluble aggregates associated with protein residues.<sup>173</sup> Hemosiderin mineral particles vary even more widely in structure than those stored in ferritin.<sup>174</sup> Allen et al identified three main particle structures in hemosiderin: a ferrihydrite-based structure, a highly defective structure based on goethite (α-FeOOH), and a noncrystalline Fe(III) structure.<sup>174</sup> The same authors found that hemosiderin particles generally have larger size distributions than particles in ferritins. As in the case of ferritins, the structural and compositional characteristics of hemosiderin vary with biological source and pathological condition.<sup>174</sup> Miyazaki et al established that denatured H-chain-rich ferritin is a major constituent of hemosiderin in the liver of patients with iron overload.<sup>175</sup>



This may be related to a decreased ability of ferritin to retain iron within its core.<sup>124,169</sup> Iron leakage from ferritin is observed also in Parkinson's disease. However, in this condition there is a pathological decrease in the concentration of ferritin L-subunits, while in NF a genetically induced mutation in the L-subunit of ferritin results in its loss of function.<sup>124</sup> Oxidative stress is considered one of the pathways leading to neuronal cell death in neurodegenerative diseases. A number of studies have aimed to assess the possible role of iron in this process, but no consensus has been reached. We refer the reader to recent papers of Collingwood et al<sup>188,189</sup> for details.

As mentioned earlier, a number of authors have considered the biomineralization of the ferrihydrite core of ferritin a possible pathway for the formation of larger magnetite particles.<sup>19,62,76,148,190–192</sup> The structure of nanocrystals in the cores of physiological horse spleen, human liver, and human brain ferritin and pathological human brain ferritin of patients with progressive supranuclear palsy and AD has been studied by electron nanodiffraction and high-resolution TEM.<sup>62</sup> A polyphase structure of the ferritin core has been postulated, but not unequivocally confirmed to date.<sup>147,193</sup> There are significant differences in the mineral composition between physiological and pathological ferritins. Although both physiological and pathological ferritin cores have a polyphase composition, hexagonal ferric iron oxide (ferrihydrite) predominates in physiological ferritin cores, while the major phases in AD brain ferritin cores are two cubic mixed ferric–ferrous iron oxides (magnetite and wüstite).<sup>62,100,148</sup>

HSFs from which iron had been gradually removed, yielding samples containing 200, 500, 1,200, and 2,200 iron atoms, were studied by TEM, XANES spectroscopy, electron energy-loss spectroscopy, small-angle X-ray scattering, and superconducting quantum-interference device (SQUID) magnetometry.<sup>154</sup> The relative amount of magnetite in ferritin containing 200–2,200 iron atoms rose steadily from approximately 20% to approximately 70%, whereas that of ferrihydrite fell from approximately 60% to approximately 20%. These results indicate a ferrihydrite–magnetite core–shell structure.<sup>154</sup>

However, these data may be questionable, as the mineral ferrihydrite is electron beam-sensitive and will undergo internal atomic rearrangements when exposed to the electron beam in TEM and scanning TEM studies, or studied by other techniques using electron beams.<sup>147,193</sup> Results obtained by nuclear magnetic resonance (NMR) relaxometry indicate that the proportion of iron contained in brain ferritin in the form of well-crystallized magnetite, rather than ferrihydrite, must be <1%,<sup>149</sup> much less than the reported percentages in the dozens of particles of a “magnetite-like” phase found

in TEM studies of similar samples.<sup>62,154</sup> Consequently, the magnetization of this “magnetite-like” phase must be very low compared with that of magnetite.<sup>149</sup> Also, recent magneto-optical and NMR studies of reconstructed and reduced HSF in aqueous solution, presented at the Tenth International Conference on the Scientific and Clinical Applications of Magnetic Carriers, indicate that high-magnetization minerals, such as magnetite or maghemite, are not present in the core of such ferritins.<sup>194</sup>

## Search for magnetoferritin in normal organs containing BMNPs

The hypothesis of the presence of a magnetically strong phase in pathological ferritin has inspired a number of experimental studies in which magnetoferritin, synthetic ferritin with a magnetic core, has been produced and investigated. However, to our best knowledge, the presence of magnetoferritin in specific human organs, serum, or cerebrospinal fluid has not been reported to date.

Various MRI methods for the estimation of iron levels in the human brain<sup>195–200</sup> are the most promising *in vivo* techniques. Also, SQUID susceptometry is being developed for the assessment of iron content in human tissues.<sup>201</sup> Of particular interest is the search for methods for the detection of magnetite in ferritin both *in vitro* and *in vivo*. Koralewski et al proposed a magneto-optical method based on the measurement of magnetic linear birefringence (MLB; Cotton–Mouton effect) followed by that of magnetic circular birefringence dispersion (Faraday rotation dispersion, or magnetic optical rotatory dispersion [MORD]) for the discrimination of the core mineral in magnetoferritin or any other MNP.<sup>139,157–160</sup> The method is depicted in Figure 11. First, MLB is measured, which allows the classification of unknown samples to a magnetically strong material, eg, magnetite or maghemite, or a magnetically weak one, eg, ferrihydrite or akaganeite (see Table 2). MLB dependence on magnetic field is very characteristic for such classes of materials, as is shown in Figure 11. For magnetically strong materials, we observe saturation of MLB, but for magnetically weak materials, typical parabolic dependence on  $H$  is observed, ie,  $\Delta n \sim H^2$ . Next, MORD measurements should be performed to obtain spectra of the studied sample. Features of MORD spectra are quite different for  $Fe^{3+}$  or  $Fe^{2+}$  ions present in studied magnetic materials (see Figure 11), so information on the oxidation state of Fe will be acquired. Taking into account results from both methods, discrimination of minerals for particular MNPs may be obtained.

Koralewski et al studied the MLB of biogenic HSF and synthetic magnetoferritin.<sup>139,160</sup> Direct observation

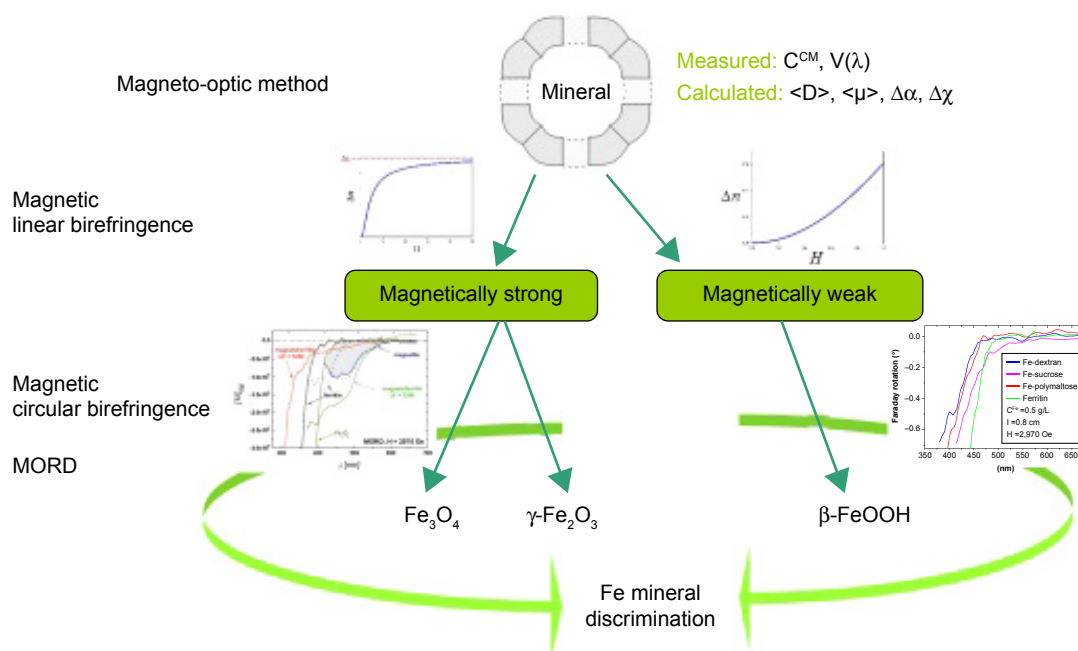


**Figure 11** Schematic representation of discrimination.

**Notes:** Based on differences in magnetic linear birefringence and MORD spectra between ferrite (magnetically strong) materials, such as magnetite/maghemite, and antiferromagnetic (magnetically weak) materials, such as ferrihydrite or akaganeite. For details of magnetically strong MORD data, see Figure 13 and Koralewski et al.<sup>159</sup> Magnetically weak MORD data were obtained for akaganeite-type materials, the same as were studied in Koralewski et al.<sup>160</sup>

**Abbreviations:** MORD, magnetic optical rotatory dispersion;  $C^{CM}$ , Cotton-Mouton constant; V, Verdet constant; D, particle diameter.

in a relatively low magnetic field has shown a saturation effect in artificial magnetoferritin, but not in HSF.<sup>139,158,160</sup> As may be seen in Figure 12, distinguishing between magnetically strong and weak materials is obvious; however, discrimination between magnetite or maghemite cores of magnetoferritin is not achieved with this single method.

Further information on the magnetic core and oxidation state of Fe can be acquired from Faraday-effect dispersion studies.<sup>159</sup> Characteristic bands of 450–478 nm are associated with magnetite NPs and magnetoferritin with a magnetite core. Observed in the visible spectrum, this feature is directly related to  $Fe^{2+}$  ions, which indicate the presence of magnetite in the studied suspension. It should be noted that  $Fe^{2+}$  ion is by definition absent in maghemite. The lack of these bands indicates a mineral other than magnetite (see Figure 13).<sup>159</sup> The characteristic band intensity may be correlated with the amount of magnetite in the studied suspension. In Figure 13, magnetoferritin with low iron content (loading factor 1,250; the same material presented in Figure 12 showing saturation of MLB) shows a very low intensity in the region of  $Fe^{2+}$  ion bands. This means that the core of this magnetoferritin consists mainly of maghemite, with a very small amount of magnetite, in contrast to highly loaded magnetoferritin

(loading factor 3,250), in which magnetite is the major component of the core.

Among the methods indicated in Table 7, Raman spectroscopy is also a very promising tool for discrimination

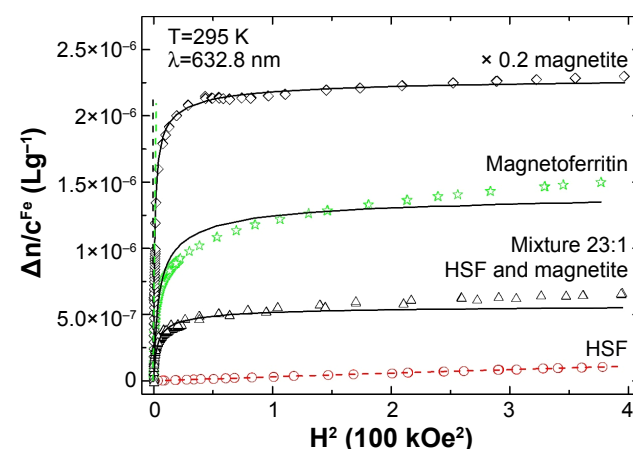


**Figure 12** Reduced linear magnetic birefringence.

**Notes:** HSF, synthetic magnetoferritin (loading factor 1,250), magnetite, and a mixture of HSF and magnetite (Fe weight proportion 23:1) versus the square of the applied magnetic field –  $H^2$ . Dashed line indicates the low-field region in which the Cotton-Mouton ( $C^{CM}$ ) constant was determined (ie,  $\Delta n = C^{CM} \lambda H^2$ , where  $\lambda$  is light wavelength and  $H$  magnetic field intensity); solid line represents the best fit for the Langevin function. Reprinted from *J Magn Magn Mater*. Vol 323. Koralewski M, Pochylski M, Mitroova Z, Timko M, Kopcansky P, Melnikova L. Magnetic birefringence of natural and synthetic ferritin. Pages 2413–2417. Copyright 2011, with permission from Elsevier.<sup>139</sup>

**Abbreviation:** HSF, horse-spleen ferritin.



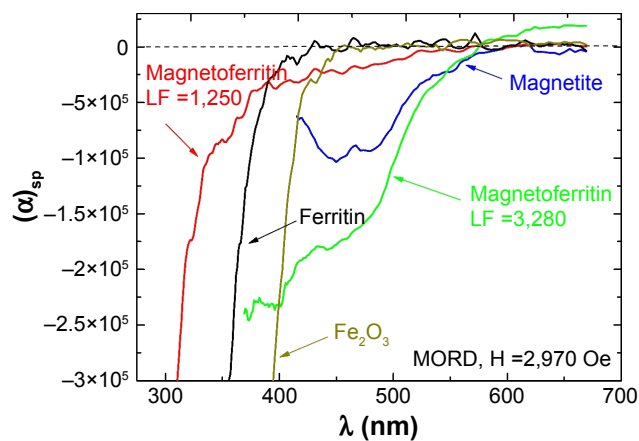


**Figure 13** Wavelength dependence.

**Notes:** Faraday rotation (MORD) for HSF, synthetic magnetoferritin with different loading factors (loading factor 1,250 and 3,280),  $\text{Fe}_2\text{O}_3$ , and magnetite suspensions. Reprinted from Koralewski M, Kłos JW, Baranowski M, et al. The Faraday effect of natural and artificial ferritins. *Nanotechnology*. 2012;23:355704. <sup>159</sup> Copyright 2012. IOP Publishing Ltd.

**Abbreviations:** MORD, magnetic optical rotatory dispersion; HSF, horse-spleen ferritin; LF, loading factor.

among different iron minerals.<sup>202</sup> Both solutions and tissue samples have been studied by this technique; we refer the reader to the latest review papers<sup>203,204</sup> for details of these studies in biological materials. Also, the recently developed MFM may be very useful in clinical analysis of biomaterials (see Figures 3 and 4).<sup>21,92,150,151</sup>

## Correlation between BMNP and ferritin distribution in human tissues

Several studies have been carried out to investigate the possible correlation between the levels of ferritin and BMNPs for the purpose of elucidating the role of ferritin in the process of BMNP biomineralization. However, elevated BMNP levels, associated with various diseases, are not necessarily correlated with increased levels of iron-storage or -transport proteins (ferritin or transferrin, respectively).<sup>20,166</sup> Magnetic materials in various human tumor tissues, including melanoma, breast, ovarian and testicle tumors, sarcoma, meningioma, glioblastoma, astrocytoma, glioma, and metastasis, were first detected by Kobayashi et al in a study using SQUID magnetometry.<sup>20</sup> However, it was impossible to demonstrate a covariance between ferritin and magnetite in that study. Investigations by magnetic methods reported by Brem et al<sup>8</sup> showed that the concentration of ferrimagnetic particles in human meningioma brain-tumor tissues was an order of magnitude higher than in nontumor hippocampus. In a comparative study of ferritin and magnetite distributions in the human brain, it has been established that magnetite is distributed homogeneously throughout the whole brain, except for the meninges, but ferritin is not.<sup>90</sup> These results suggest

that magnetite in the human brain and tumor tissues does not originate from ferritin;<sup>20</sup> however, further experimental documentation is necessary to confirm this conclusion.

## Comparison between size distributions of clumps of biogenic magnetite and ferritin aggregates

Measurements of the size distribution of BMNPs and aggregates of pathological ferritin do not confirm the hypothesis that ferritin might be a precursor of BMNPs either.<sup>170,205</sup> Biogenic magnetite observed in brain tissues<sup>97,192,206,207</sup> has a wide particle-size range, including both SPM and larger magnetite particles (clump magnetite) with a size of 10–200 nm. Larger particles were observed in tissue extracts; optical microscopy studies revealed 5–10  $\mu\text{m}$  clusters of finer opaque particles in tissue slices.<sup>205</sup> The magnetite-clump level measured in NF tissue was 57 and 128 ng/g wet tissue, higher than that normally measured in age/sex-matched freeze-dried control tissues from the same region of the brain (12–27 ng/g wet tissue).<sup>170</sup> The observed nontrivial magnetization corresponds to clumps of magnetite with a coercivity larger than 200 Oe, which is consistent with the results of isothermal remnant-magnetization measurements, indicative of magnetite clumps.<sup>170</sup> Also coercivity data reported by Hautot et al<sup>170</sup> and TEM imaging of magnetic extracts from hippocampal tissue<sup>205</sup> indicate the presence of larger clumps of magnetite particles. Moreover, the ferrihydrite core of ferritin is superantiferromagnetic,<sup>137</sup> and the saturation magnetization of ferritin proves unattainable, even in a field as strong as 550 kOe.<sup>140,141</sup> Therefore, direct formation of BMNPs from the ferrihydrite core of ferritin is impossible. Also the origin of large clumps of magnetite crystals (BMNPs) remains unclear, according to Hautot et al,<sup>170</sup> because of the inconsistency in size distribution and magnetic properties between clumps of biogenic magnetite and ferritin aggregates.

## Biological formation of BMNPs in vitro

There are a number of papers on the influence of MTB proteins involved in BMNP biomineralization on the formation of magnetite nanocrystals in vitro.<sup>208,209</sup> For example, the magnetosome-membrane protein Mms6 has allowed the artificial control of the morphology, crystallinity, and magnetism of nanocrystals in a manner observed in MTB.<sup>209–211</sup> To investigate the conditions of biological formation of magnetite nanocrystals, Prozorov et al precipitated iron oxide in an aqueous viscous Pluronic solution of Fe(II) and Fe(III) by increasing the pH in the presence of various proteins.<sup>208</sup> A protein isolated from magnetosome membranes mediated

the formation of 30 nm-large magnetite crystals with good crystallinity; NPs formed within ferritin under the same conditions were much smaller and largely amorphous<sup>208</sup> (NP growth within the ferritin core is limited by the protein shell; see Figure 8). Nanocrystals formed in the presence of ferritin do not have uniform sizes and shapes, in contrast to those produced in the presence of the biomineralization protein Mms6.<sup>208</sup> A protein assisting magnetite production, MamP has been established recently<sup>212</sup> as an iron oxidase contributing to the formation of Fe(III) ferrihydrite. As such, this protein will be the next candidate for in vitro testing.

## Genetic analysis of role of ferritin in BMNP biomineralization

The elucidation of the physiological origin of BMNPs in eukaryotes, including humans, is still more complex because of the difficulties in the detection of BMNPs in human tissues. Finding magnetite in tissue is a nontrivial problem, due to its low concentrations, of the order of dozens of ng/g tissue. A powerful tool in this field is provided by bioinformatic methods based on comparative genomics. These bioinformatic methods are complementary to physical methods. The sophisticated physical methods for BMNP detection (Table 7) do not always allow the distinction of BMNPs from artificial MNPs in human tissues in contact with the environment. Also, by using only physical methods, it is often difficult to distinguish extracellular biomineralization of MNPs by microorganisms from their biosorption from the environment.<sup>116</sup>

As we have mentioned, the genetic mechanism of BMNP biomineralization is predicted to be based on homologues of MTB magnetosome-island proteins indispensable for the biomineralization of BMNPs in MTB.<sup>23,213,214</sup> However, the question remains open as to whether ferritin also, together with homologues of MTB magnetosome-island proteins, is involved in the metabolic pathway of BMNP biomineralization. An answer has been proposed<sup>214</sup> on the basis of comparative genomic studies. To this end, ferritin-encoding genes were searched for full genomes of MTB.<sup>108,113,215–218</sup> Gorobets et al<sup>214</sup> demonstrated that the magnetotactic bacterium *Magnetococcus marinus* MC1 had no genes encoding ferritin or ferritin-like proteins in their full genomes.

Research<sup>214</sup> has led to the conclusion that the presence of ferritin in cells of MTB is not necessary for the biomineralization of BMNPs, that ferrihydrite in ferritin is not a precursor of biogenic magnetite in MTB, and that prokaryotes and eukaryotes have a common genetic mechanism of biomineralization of intracellular BMNPs.<sup>23,213,214</sup> In general,

ferrihydrite in the ferritin core is not a precursor of BMNPs in humans or other multicellular organisms. As mentioned, this has been confirmed by an experimental study of conditions of magnetite biomineralization in vitro.<sup>208</sup>

These findings of bioinformatic studies are in accordance with the aforementioned experimental data on the lack of correlation between BMNP and ferritin distributions in human tissues, and the inconsistency in size distribution between clumps of biogenic magnetite and ferritin aggregates. In this context, the bioinformatic analysis in the paper<sup>214</sup> proves that the biomineralization of BMNPs is in general a process independent of iron storage in the core of ferritin and ferritin-like proteins. However, in our opinion, an excess of labile iron related to the decreased ability of ferritin to retain iron within its core in pathological conditions<sup>123,169</sup> may represent an additional iron supply for BMNP biomineralization. Besides, the biomineralization of BMNPs can protect tissues against oxidative stress, since iron in magnetite is bound irreversibly and cannot be released for the Fenton reaction.<sup>219</sup> In this regard, iron storage in organisms can be classified as either reversible (in iron-storage proteins) or irreversible (in BMNPs).

Metals accumulated in AD and other neurodegenerative disorders are known to include (besides iron) such elements as copper or zinc.<sup>220,221</sup> The accumulation of copper and zinc can be explained by a common genetic mechanism of BMNP biomineralization, since the proteins indispensable for BMNP biomineralization include divalent cation ( $Zn^{+2}$ ,  $Cu^{+2}$ ,  $Cd^{+2}$ ,  $Ni^{+2}$ , and  $Fe^{+2}$ ) transporters. Therefore, Co, Ni, Zn, Cu, Mn, and Cd can be incorporated in the magnetite structure<sup>211,222</sup> and bound irreversibly in BMNP biomineralization. On the other hand, purified ferritin cages in vitro can incorporate a variety of metal ions (Fe, Au, Pd, Rh, Pt, Ni, Cr, Cd, Ti, Tb, Co, Cu, and Zn), most likely through a hydrophilic threefold ion channel.<sup>183,223,224</sup> Therefore, both ferritin and BMNPs might contribute to the excess of zinc and copper in neurodegenerative disorders.<sup>225</sup>

## Conclusion and prospects

In this review, we have outlined the research efforts toward understanding the biomineralization of BMNPs and especially their role in human health and disease. In general, three basic steps can be distinguished in BMNP biomineralization in organisms of all three domains (prokaryotes, archaea, and eukaryotes, including humans): 1) formation of a specific organic material, organic matrix, or vesicle to prepare a chemical medium favorable for BMNP biomineralization; 2) formation of a transient iron mineral; and

3) conversion of the transient iron-mineral precursor into the target BMNP mineral.

Each of these steps requires the participation of a set of specific proteins. The formation of an organic matrix or other organic surroundings of BMNPs involves proteins that are not homologues of those controlling the formation of vesicles in MTB.<sup>23,115</sup> Steps 2 and 3 are predicted to be controlled by homologues of MTB biomineralization proteins.<sup>23,115</sup>

Ferrihydrite is the most probable transient mineral and precursor of biogenic magnetite.<sup>9,214</sup> However, the accumulation of iron in BMNP biomineralization and the accumulation of iron in the ferrihydrite core of ferritin are independent processes in general.<sup>9,214</sup> The role of ferritin in BMNP biomineralization remains an open question. In diseases and mutations, an increase in labile iron due to the reduced ability of ferritin to retain iron within its core can influence the process of biomineralization of BMNPs. There are two modes of iron storage in living organisms: reversible storage in iron-storage proteins, and irreversible storage in BMNPs, in which iron is bound in magnetite or other chemically resistant iron oxides and cannot be released. Since ferrites represent the most magnetically sensitive compounds of biogenic origin and elevated BMNP levels are related to a number of human diseases, such as cancer, neurodegenerative disorders, or atherosclerosis, the study of the influence of magnetic fields on the expression of genes encoding biomineralization proteins<sup>226,227</sup> is of key importance in the investigation of the influence of magnetic fields on living organisms.

The discovery of BMNPs in organisms of all three domains – prokaryotes, archaea, and eukaryotes – and the observed peculiarities of their formation in health and disease have prompted the investigation of their metabolic functions. Controlled application of weak static magnetic fields may cause rotation of SD magnetite, which may result in the opening of ionic membrane channels, modulation of the transmembrane potential, and/or generation of action potentials in neurons.<sup>48,228</sup> Simulations performed by Jandacka et al<sup>229</sup> show that SPM ferritin molecules cannot be deformed or rotated in weak geomagnetic fields, and thus cannot be involved in magnetoreception by deformation. Furthermore, there is an alternative hypothesis that ferritin molecules in the avian ear may function as intracellular electromagnetic oscillators, generating additional electrical fields with an amplitude of ~0.1 pV in receptor cells and consequently auditory neurons.<sup>229</sup> However, we think that a voltage of 0.1 pV is too low to produce any significant biological effect, since the working membrane voltages are of the order of dozens of millivolts. There is also a hypothesis that

BMNP chains represent nanoscale high-gradient magnetic separators of cluster components (eg, vesicles, granules, cells) in organisms.<sup>229–231</sup>

We hope that further development of physical methods for the discrimination of the core minerals in ferritin in physiological fluids and/or tissue will provide powerful tools to fight neurodegenerative disorders. In this regard, we think that the magnetism of the ferritin core may be a useful prognostic indicator, especially in some neurodegenerative diseases. Better understanding of core mineral content and its composition and also tissue–organ distribution of ferritin will certainly help in clarifying the etiology of several diseases. This calls for an intensification of research into the magnetic properties of ferritin from different organs (see Figure 8) from healthy and pathological human subjects. The mapping of ferritin and BMNP in different organs and especially the brain would be very important, and not only from the clinical analytical point of view. Such studies may shed new light on long-term memory in which it is believed magnetite can be involved.<sup>232,233</sup> Recent studies by the Kirschvink group<sup>234</sup> on possible human magnetic sensing await further proof, and many questions remain unanswered.

## Acknowledgments

We appreciate the reviewer's comments, which improved our manuscript. This project received funding from the European Union's Horizon 2020 Research and Innovation program under a Marie Skłodowska-Curie grant (agreement 644348 [MagIC]). We would like to thank M Molcan (SAS Košice) for growing MTB and B Leszczyński (Adam Mickiewicz University, Poznań) for providing TEM of MTB.

## Disclosure

The authors report no conflicts of interest in this work.

## References

1. Meldrum FC, Cölfen H. Controlling mineral morphologies and structures in biological and synthetic systems. *Chem Rev*. 2008;108:4332–4432.
2. Eherlich H. Biomineralization special issue. *Acta Biomater*. 2014;10:3813–3814.
3. Mann S. *Biomineralization: Principles and Concepts in Bioorganic Materials Chemistry*. New York: Oxford University Press; 2001.
4. Blakemore R. Magnetotactic bacteria. *Science*. 1975;190:377–379.
5. Frankel RB, Blakemore RP, Wolfe RS. Magnetite in freshwater magnetotactic bacteria. *Science*. 1979;203:1355–1356.
6. Sakaguchi T, Burgess JG, Matsunaga T. Magnetite formation by a sulphate-reducing bacterium. *Nature*. 1993;365:47–49.
7. Mann S, Sparks NH, Frankel RB, Bazylinski DA, Jannasch HW. Biomineralization of ferrimagnetic greigite (Fe<sub>3</sub>S<sub>4</sub>) and iron pyrite (FeS<sub>2</sub>) in a magnetotactic bacterium. *Nature*. 1990;343:258–261.
8. Brem F, Hirt AM, Winklhofer M, et al. Magnetic iron compounds in the human brain: a comparison of tumor and hippocampal tissue. *J R Soc Interface*. 2006;3:833–841.

9. Faivre D, Godec TU. From bacteria to mollusks: the principles underlying the biomineralization of iron oxide materials. *Angew Chem Int Ed Engl*. 2015;54:4728–4747.
10. Qin SY, Yin H, Yang CL, et al. A magnetic protein biocompass. *Nat Mater*. 2016;15:217–226.
11. Richter M, Kube M, Bazylinski DA, et al. Comparative genome analysis of four magnetotactic bacteria reveals a complex set of group-specific genes implicated in magnetosome biomineralization and function. *J Bacteriol*. 2007;189:4899–4910.
12. Abreu F, Cantão ME, Nicolás MF, et al. Common ancestry of iron oxide- and iron-sulfide-based biomineralization in magnetotactic bacteria. *ISME J*. 2011;5:1634–1640.
13. Komeili A, Li Z, Newman DK, Jensen GJ. Magnetosomes are cell membrane invaginations organized by the action-like protein MamK. *Science*. 2006;311:242–245.
14. Komeili A. Molecular mechanisms of magnetosome formation. *Annu Rev Biochem*. 2007;76:351–366.
15. Komeili A. Molecular mechanisms of compartmentalization and biomineralization in magnetotactic bacteria. *FEMS Microbiol Rev*. 2012;36:232–255.
16. Pankhurst Q, Hautot D, Khan N, Dobson J. Increased levels of magnetic iron compounds in Alzheimer's disease. *J Alzheimers Dis*. 2008;13:49–52.
17. Brem F, Hirt AM, Simon C, Wieser HG, Dobson J. Characterization of iron compounds in tumour tissue from temporal lobe epilepsy patients using low temperature magnetic methods. *Biometals*. 2005;18:191–197.
18. Bartzokis G, Tishler TA, Lu PH, et al. Brain ferritin iron may influence age- and gender-related risk of neurodegeneration. *Neurobiol Aging*. 2007;28:414–423.
19. Hautot D, Pankhurst QA, Khan N, Dobson J. Preliminary evaluation of nanoscale biogenic magnetite and Alzheimer's disease. *Proc Biol Sci*. 2003;270:S62–S64.
20. Kobayashi A, Yamamoto N, Kirschvink J. Studies of inorganic crystals in biological tissue: magnetite in human tumor. *J Jpn Soc Powder Powder Metall*. 1997;44:294–300.
21. Chekchun VF, Gorobets S, Gorobets O, Demianenko IV. Magnet-sensitive nanostructures of endogenous origin in Ehrlich carcinoma cells. *Nanostruct Mater*. 2011;2:102–109.
22. Kobayashi A, Yamamoto N, Kirschvink J. Study of inorganic crystalline solids in biosystems: magnetite in the human body. *J Soc Powder and Powder Metall*. 1996;43:1354–1360.
23. Gorobets O, Gorobets S, Gorobets Y. Biogenic magnetic nanoparticles: biomineralization in prokaryotes and eukaryotes. In: Lyshevski SE, editor. *Dekker Encyclopedia of Nanoscience and Nanotechnology*. 3rd ed. New York: CRC Press; 2014:300–308.
24. Grünberg K, Müller E, Otto A, et al. Biochemical and proteomic analysis of the magnetosome membrane in *Magnetospirillum gryphiswaldense*. *Appl Environ Microbiol*. 2004;70:1040–1050.
25. Arakaki A, Nakazawa H, Nemoto M, Mori T, Matsunaga T. Formation of magnetite by bacteria and its application. *J R Soc Interface*. 2008;5:977–999.
26. Komeili A, Vali H, Beveridge TJ. Magnetosome vesicles are present before magnetite formation, and MamA is required for their activation. *Proc Natl Acad Sci U S A*. 2004;101:3839–3844.
27. Fukumori Y, Oyanagi H, Yoshimatsu K. Enzymatic iron oxidation and reduction in magnetite synthesizing *Magnetospirillum magnetotacticum*. *J Phys IV France*. 1997;7:659–662.
28. Prozorov T. Magnetic microbes: bacterial magnetite biomineralization. *Semin Cell Dev Biol*. 2015;46:36–43.
29. Devouard B, Pósfai M, Hua X, Bazylinski DA, Frankel RB, Buseck PR. Magnetite from magnetotactic bacteria: size distributions and twinning. *Am Mineralogist*. 1998;83:1387–1398.
30. Tanaka M, Mazugama E, Avahaki A, Matsunaga T. MMS6 protein regulates crystal morphology during nano-sized magnetite biomineralization in vivo. *J Biol Chem*. 2011;286:6386–6392.
31. Naresh M, Hasija V, Sharma M, Mittal A. Synthesis of cellular organelles containing nano-magnets stunts growth of magnetotactic bacteria. *J Nanosci Nanotechnol*. 2010;10:4135–4144.
32. Thomas-Keprta KL, Bazylinski DA, Kirschvink JL, et al. Elongated prismatic magnetite crystals in ALH84001 carbonate globules: potential Martian magnetofossils. *Geochim Cosmochim Acta*. 2000;64:4049–4081.
33. Hsu CY, Ko FY, Li CW, Fann K, Lue JT. Magnetoreception system in honeybees (*Apis mellifera*). *PLoS One*. 2007;4:e395.
34. Maher BA. Magnetite biomineralization in termites. *Proc Biol Sci*. 1998;265:733–737.
35. Cranfield CG, Dawe A, Karloukovski V, Dunin-Borkowski RE, de Pomerai D, Dobson J. Biogenic magnetite in the nematode *Caenorhabditis elegans*. *Proc Biol Sci*. 2004;271:436–439.
36. Mann S, Sparks NH, Walker MM, Kirschvink JL. Ultrastructure, morphology and organization of biogenic magnetite from sockeye salmon, *Oncorhynchus nerka*: implications for magnetoreception. *J Exp Biol*. 1988;140:35–49.
37. Wiltshchko R, Wiltshchko W. *Magnetic Orientation in Animals*. Berlin: Springer; 1995.
38. Walcott C, Gould JL, Kirschvink JL. Pigeons have magnets. *Science*. 1979;184:180–182.
39. Vainshtein M, Suzina N, Kudryashova E, Ariskina E. New magnet-sensitive structures in bacterial and archaeal cells. *Biol Cell*. 2002;94:29–35.
40. Gajdardziska-Josifovska M, McClean RG, Schofield MA, Sommer CV, Kean WF. Discovery of nanocrystalline biogenic magnetite. *Eur J Mineral*. 2001;13:863–870.
41. de Barros HG, Esquivel DM, Danon J, de Oliveira LP. Magnetotactic algae. *An Acad Bras Cienc*. 1982;54:257–258.
42. Suzukia Y, Kopp RE, Kogure T, et al. Sclerite formation in the hydrothermal-vent “scaly-foot” gastropod: possible control of iron sulfide biomineralization by the animal. *Earth Planet Sci Lett*. 2006;242:39–50.
43. de Oliveira JF, Wajnberg E, Esquivel DM, Weinkauff S, Winklhofer M, Hanzlik M. Ant antennae: are they sites for magnetoreception? *J R Soc Interface*. 2010;7:143–152.
44. Gould JL, Kirschvink JL, Deffeyes KS. Bees have magnetic remanence. *Science*. 1978;202:1026–1028.
45. Acosta-Avalos D, Wajnberg E, Oliveira PS, Leal I, Farina M, Esquivel DM. Isolation of magnetic nanoparticles from *Pachycondyla marginata* ants. *J Exp Biol*. 1999;202:2687–2692.
46. Lohmann KJ. Magnetic remanence in the western Atlantic spiny lobster, *Panulirus argus*. *J Exp Biol*. 1984;113:29–41.
47. Brassart J, Kirschvink JL, Phillips JB, Borland SC. Ferromagnetic material in the eastern red-spotted newt *Notophthalmus viridescens*. *J Exp Biol*. 1999;202:3155–3160.
48. Kirschvink JL. Magnetite biomineralization and geomagnetic sensitivity in higher animals: an update and recommendations for future study. *Bioelectromagnetics*. 1989;10:239–259.
49. Diebel CE, Proksch R, Green CR, Walker MM. Magnetite defines a vertebrate magnetoreceptor. *Nature*. 2000;406:299–302.
50. Eder SH, Cadiou H, Muhamad A, McNaughton PA, Kirschvink JL, Winklhofer M. Magnetic characterization of isolated candidate vertebrate magnetoreceptor cell. *Proc Natl Acad Sci U S A*. 2012;109:12022–12027.
51. Moore A, Freahe SM, Thomas IM. Magnetic particles in the lateral line of the Atlantic salmon (*Salmo salar* L.). *Philos Trans R Soc Lond B Biol Sci*. 1990;329:11–15.
52. Moore A, Riley WD. Magnetic particles associated with the lateral line of the European eel *Anguilla anguilla*. *J Fish Biol*. 2009;74:1629–1634.
53. Oguram M, Katom M, Arain N, Sasadat T, Sakakya Y. Magnetic particles in chum salmon (*Oncorhynchus keta*): extraction and transmission electron microscopy. *Can J Zool*. 1992;70:874–877.
54. Irwin WP, Lohmann KJ. Disruption of magnetic orientation in hatchling loggerhead sea turtles by pulsed magnetic fields. *J Comp Physiol A Neuroethol Sens Neural Behav Physiol*. 2005;191:475–480.
55. Falkenberg G, Fleissner G, Schuchardt K, et al. Avian magnetoreception: elaborate iron mineral containing dendrites in the upper beak seem to be a common feature of birds. *PLoS One*. 2010;5:e9231.



56. Fleissner G, Fleissner G, Stahl B, Falkenberg G. Iron-mineral-based magnetoreception in birds: the stimulus conducting system. *J Ornithol*. 2003;148:S643–S648.
57. Edwards HH, Schnell GD, DuBois RL, Hutchison VH. Natural and induced remanent magnetism in birds. *Auk*. 1992;109:43–56.
58. Edelman NB, Fritz T, Nimp S, et al. No evidence for intracellular magnetite in putative vertebrate magnetoreceptors identified by magnetic screening. *Proc Natl Acad Sci U S A*. 2015;112:262–267.
59. Holland RA, Kirschvink JL, Doak TG, Wikelski M. Bats use magnetite to detect the earth's magnetic field. *PLoS One*. 2008;3:e1676.
60. Zoeger J, Dunn JR, Fuller M. Magnetic material in the head of the common Pacific dolphin. *Science*. 1981;213:892–894.
61. Kirschvink JL, Kobayashi-Kirschvink A, Woodford BJ. Magnetite biomineralization in the human brain. *Proc Natl Acad Sci U S A*. 1992;89:7683–7687.
62. Quintana C, Cowley JM, Marhic C. Electron nanodiffraction and high-resolution electron microscopy studies of the structure and composition of physiological and pathological ferritin. *J Struct Biol*. 2004;147:166–178.
63. Collingwood J, Chong RK, Kasama T, et al. Three-dimensional tomographic imaging and characterization of iron compounds within Alzheimer's plaque core material. *J Alzheimers Dis*. 2008;14:235–245.
64. Grassi-Schultheiss PP, Heller F, Dobson J. Analysis of magnetic material in the human heart, spleen and liver. *Biometals*. 1997;10:351–355.
65. Kirschvink JL. Ferromagnetic crystals (magnetite?) in human tissue. *J Exp Biol*. 1981;92:333–335.
66. Schultheiss-Grassi PP, Dobson J. Magnetic analysis of human brain tissue. *Biometals*. 1999;12:67–72.
67. Pósfai M, Dunin-Borkowski RE. Magnetic nanocrystals in organisms. *Elements*. 2009;5:235–240.
68. Kirschvink JL, Kobayashi-Kirschvink A, Diaz-Ricci JC, Kirschvink SJ. Magnetite in human tissues: a mechanism for the biological effects of weak ELF magnetic fields. *Bioelectromagnetics*. 1992;1 Suppl: 101–113.
69. Bazylinski DA, Frankel RB. Magnetosome ferritin in prokaryotes. *Nat Rev Microbiol*. 2004;2:217–230.
70. Faivre D, Schüler D. Magnetotactic bacteria and magnetosomes. *Chem Rev*. 2008;108:4875–4898.
71. Schüler D. *Magnetoreception and Magnetosomes in Bacteria*. Heidelberg: Springer; 2007.
72. Lowenstam HA. Magnetite in denticle capping in recent chitons (Polyplacophora). *Geol Soc Am Bull*. 1962;73:435–438.
73. Walker MM, Kirschvink JL, Chang SB, Dizon AE. A candidate magnetic sense organ in the yellowfin tuna, *Thunnus albacares* Science. 1984;224:751–753.
74. Hanzlik M, Heunemann C, Holtkamp-Rötzler E, Winklhofer M, Petersen N, Fleissner G. Superparamagnetic magnetite in the upper beak tissue of homing pigeons. *Biometals*. 2000;13:325–331.
75. Cadiou H, McNaughton PA. Avian magnetite-based magnetoreception: a physiologist's perspective. *J R Soc Interface*. 2010;7:S193–S205.
76. Collingwood JF, Mikhaylova A, Davidson M, et al. In situ characterization and mapping of iron compounds in Alzheimer's disease tissue. *J Alzheimers Dis*. 2005;7:267–272.
77. Dunlop DJ, Özdemir Ö. *Rock Magnetism: Fundamentals and Frontiers*. Cambridge: Cambridge University Press; 1997.
78. Muxworthy AR, Williams W. Critical superparamagnetic/single-domain grain sizes in interacting magnetite particles: implications for magnetosome crystals. *J R Soc Interface*. 2009;6:1207–1212.
79. Lins U, McCartney MR, Farina M, Frankel RB, Buseck PR. Habits of magnetosome crystals in coccoid magnetotactic bacteria. *Appl Environ Microbiol*. 2005;71:4902–4905.
80. Muxworthy AR, Williams W. Critical single domain/multidomain grain-sizes in non-interacting and interacting elongated magnetite particles: implications for magnetosomes. *J Geophys Res*. 2006;111: B12S12.
81. Goss CJ. Saturation magnetisation, coercivity and lattice parameter changes in the system  $\text{Fe}_3\text{O}_4$ - $\gamma\text{Fe}_2\text{O}_3$ , and their relationship to structure. *Phys Chem Miner*. 1988;16:164–171.
82. Kletetschka G, Wasilewski PJ, Taylor PT. Hematite vs. magnetite as the signature for planetary magnetic anomalies? *Phys Earth Planet Inter*. 2000;119:259–267.
83. Pannalal SJ, Crowe SA, Cioppa MT, Symons DT, Sturm A, Fowle DA. Room-temperature magnetic properties of ferrihydrite: a potential magnetic remanence carrier? *Earth Planet Sci Lett*. 2005;236:856–870.
84. Cornell MR, Schwertmann U. *The Iron Oxides: Structure, Properties, Reactions, Occurrences and Uses*. Weinheim, Germany: Wiley; 2004.
85. Roberts AP, Chang L, Rowan CJ, Horng CS, Florindo F. Magnetic properties of sedimentary greigite ( $\text{Fe}_3\text{S}_4$ ): an update. *Rev Geophys*. 2011;49: RG1002.
86. Felner I, Alenkina IV, Vinogradov AV, Oshtrakh MJ. Peculiar magnetic observations in pathological human liver. *J Magn Magn Mater*. 2016; 399:118–122.
87. Dubiel SM, Zabłotna-Rypien B, Mackey JB. Magnetic properties of human liver and brain ferritin. *Eur Biophys J*. 1999;28:263–267.
88. Baker RR, Mather JG, Kennaugh JH. Magnetic bones in human sinuses. *Nature*. 1983;303:78–80.
89. Collingwood J, Dobson J. Mapping and characterization of iron compounds in Alzheimer's tissue. *J Alzheimers Dis*. 2006;10:215–222.
90. Chen J, Hardy PA, Clauberg M, et al. T2 values in the human brain: comparison with quantitative assays of iron and ferritin. *Radiology*. 1989; 173:521–526.
91. Schultheiss-Grassi PP, Wessiken R, Dobson J. TEM observation of biogenic magnetite extracted from the human hippocampus. *Biochim Biophys Acta*. 1999;1426:212–216.
92. Alekseeva TA, Gorobets S, Gorobets O, Demyanenko IV, Lazarenko OM. Magnetic force microscopy of atherosclerotic plaque. *Med Perspect*. 2014;1:4–10.
93. Moos T, Morgan EH. The metabolism of neuronal iron and its pathogenic role in neurological disease: review. *Ann N Y Acad Sci*. 2004; 1012:14–26.
94. Bartzokis G, Tishler TA. MRI evaluation of basal ganglia ferritin iron and neurotoxicity in Alzheimer's and Huntington's disease. *Cell Mol Biol (Noisy-le-grand)*. 2000;46:821–833.
95. Lovell MA, Robertson JD, Teesdale WJ, Campbell JL, Markesbery WR. Copper, iron and zinc in Alzheimer's disease senile plaques. *J Neurol Sci*. 1998;158:47–52.
96. Collingwood JF, Mikhaylova A, Davidson MR, et al. High-resolution X-ray absorption spectroscopy studies of metal compounds in neurogenerative brain tissue. *J Phys Conf Ser*. 2005;17:54–60.
97. Dobson J. Investigation of age-related variations in biogenic magnetite levels in the human hippocampus. *Exp Brain Res*. 2002;144: 122–126.
98. Fuller M, Dobson J, Wieser HG, Moser S. On the sensitivity of the human brain to magnetic fields: evocation of epileptiform activity. *Brain Res Bull*. 1995;36:155–159.
99. Plascencia-Villa G, Ponce A, Collingwood JF, et al. High-resolution analytical imaging and electron holography of magnetite particles in amyloid cores of Alzheimer's disease. *Sci Rep*. 2016;6:24873.
100. Quintana C, Bellefqih S, Laval JY, et al. Study of the localization of iron, ferritin, and hemosiderin in Alzheimer's disease hippocampus by analytical microscopy at the subcellular level. *J Struct Biol*. 2006; 153:42–54.
101. Teller S, Tahirbegi IB, Mir M, Samitier J, Soriano J. Magnetite-amyloid- $\beta$  deteriorates activity and functional organization in an in vitro model for Alzheimer's disease. *Sci Rep*. 2015;5:17261.
102. Gieré R. Magnetite in the human body: biogenic vs. anthropogenic. *Proc Natl Acad Sci U S A*. 2016;113:11986–11987.
103. Maher BA, Ahmed IA, Karloukovski V, et al. Magnetite pollution nanoparticles in the human brain. *Proc Natl Acad Sci U S A*. 2016;113: 10797–10801.
104. Felfoul O, Mohammadi M, Taherkhani S, et al. Magneto-aerotactic bacteria deliver drug-containing nanoliposomes to tumour hypoxic regions. *Nat Nanotechnol*. 2016;11:941–947.
105. Gorobets S, Gorobets O, Butenko K, Chizh YM. Biomineralization of magnetic nanoparticles by bacterial symbionts of human. *Med Perspect*. 2014;19:4–12.

106. Elfick A, Rischitor G, Mouras R, et al. Biosynthesis of magnetic nanoparticles by human mesenchymal stem cells following transfection with the magnetotactic bacterial gene *mms6*. *Sci Rep*. 2017;7: 39755.
107. Ullrich S, Kube M, Schübbe S, Reinhardt R, Schüler D. A hypervariable 130-kilobase genomic region of *Magnetospirillum gryphiswaldense* comprises a magnetosome island which undergoes frequent rearrangements during stationary growth. *J Bacteriol*. 2005;187:7176–7184.
108. Schübbe S, Williams TJ, Xie G, et al. Complete genome sequence of the chemolithoautotrophic marine magnetotactic coccus strain MC-1. *Appl Environ Microbiol*. 2009;75:4835–4852.
109. Murat D, Quinlan A, Vali H, Komeili A. Comprehensive genetic dissection of the magnetosome gene island reveals the step-wise assembly of a prokaryotic organelle. *Proc Natl Acad Sci U S A*. 2010;107: 5593–5598.
110. Zeytuni N, Ozyamak E, Ben-Harush K, et al. Self-recognition mechanism of MamA, a magnetosome-associated TPR-containing protein, promotes complex assembly. *Proc Natl Acad Sci U S A*. 2011;108: E480–E487.
111. Scheffel A, Gärdes A, Grünberg K, Wanner G, Schüler D. The major magnetosome proteins MamGFDC are not essential for magnetite biomineralization in *Magnetospirillum gryphiswaldense* but regulate the size of magnetosome crystals. *J Bacteriol*. 2008;190:377–386.
112. Lohe A, Ullrich S, Katzmann E, et al. Functional analysis of the magnetosome island in *Magnetospirillum gryphiswaldense*: the mamAB operon is sufficient for magnetite biomineralization. *PLoS One*. 2011;6:e25561.
113. Grünberg K, Wawer C, Tebo BM, Schüler D. A large gene cluster encoding several magnetosome proteins is conserved in different species of magnetotactic bacteria. *Appl Environ Microbiol*. 2001;67: 4573–4582.
114. Weddemann A, Ennen I, Regtmeier A, et al. Review and outlook: from single nanoparticles to self-assembled monolayers and granular GMR sensors. *Beilstein J Nanotechnol*. 2010;1:75–93.
115. Gorobets O, Gorobets S, Gorobets Y. Biomineralization of intracellular biogenic magnetic nanoparticles and their possible functions. *Res Bull NTUU*. 2013;3:28–33.
116. Gorobets O, Gorobets S, Sorokina L. Biomineralization and synthesis of biogenic magnetic nanoparticles and magnetosensitive inclusions in microorganisms and fungi. *Funct Mater*. 2014;21:427–436.
117. Wang H, Yu YF, Sun YB, Chen QW. Magnetic nanochains: a review. *Nano*. 2011;6:1–17.
118. Gorobets S, Gorobets O, Demyanenko IV. Self-organization of magnetite nanoparticles in providing *Saccharomyces cerevisiae* yeasts with magnetic properties. *J Magn Magn Mater*. 2013;337:53–57.
119. Jordan VC, Caplan M, Bennett KM. Simplified synthesis and relaxometry of magnetoferritin for magnetic resonance imaging. *Magn Res Med*. 2010;64:1260–1266.
120. Figuerola A, Di Corato R, Manna L, Pellegrino T. From iron oxide nanoparticle towards advanced iron-based inorganic materials designed for biomedical applications. *Pharmacol Res*. 2010;62:126–143.
121. Knovich MA, Storey JA, Coffman LG, Torti SV, Torti FM. Ferritin for the clinician. *Blood Rev*. 2009;23:95–104.
122. Quintana C, Gutiérrez L. Could dysfunction of ferritin be a determinant factor in the aetiology of some neurodegenerative diseases? *Biochim Biophys Acta*. 2010;1800:770–782.
123. Double KL, Maywald M, Schmitt M, Reiderer P, Gerlach M. In vitro studies of ferritin iron release and neurotoxicity. *J Neurochem*. 1998;70:2492–2499.
124. Friedman A, Arosio P, Finazzi D, Koziorowski D, Galazka-Friedman J. Ferritin as an important player in neurodegeneration. *Parkinsonism Relat Disord*. 2011;17:423–430.
125. Laufberger V. Sur la cristallization de la ferritine. *Bull Soc Chim Biol*. 1937;19:1575–1582.
126. Harrison PM, Arosio P. The ferritins: molecular properties, iron storage function and cellular regulation. *Biochim Biophys Acta*. 1996;1275: 161–203.
127. Thiel E. Ferritin: structure, gene regulation, and cellular function in animals, plants and microorganisms. *Annu Rev Biochem*. 1987;56: 289–315.
128. Ebrahimi KH, Hagedoorn PL, Hagen WR. Unity in the biochemistry of the iron-storage proteins ferritin and bacterioferritin. *Chem Rev*. 2015;115:295–326.
129. Jutz G, van Rijn P, Miranda BS, Böker A. Ferritin: a versatile building block for bionanotechnology. *Chem Rev*. 2015;115:1653–1701.
130. Finazzi D, Arosio P. Biology of ferritin in mammals: an update on iron storage, oxidative damage and neurodegeneration. *Arch Toxicol*. 2014;88:1787–1802.
131. Zhao G. Phytoferritin and its implications for human health and nutrition. *Biochim Biophys Acta*. 2010;1800:815–823.
132. Almiron M, Link AJ, Furlong D, Kolter R. A novel DNA-binding protein with regulatory and protective roles in starved *Escherichia coli*. *Genes Dev*. 1992;6:2646–2654.
133. Lewin A, Moore GR, Le Brun NE. Formation of protein-coated iron minerals. *Dalton Trans*. 2005:3597–3610.
134. Levi S, Cozzi A, Arosio P. Neuroferritinopathy: a neurodegenerative disorder associated with L-ferritin mutation. *Best Pract Res Clin Haematol*. 2005;18:265–276.
135. Hastings NA, Peacock JB. *Statistical Distributions*. London: Butterworth; 1975.
136. Popplewell J, Sakhnini L. The dependence of the physical and magnetic properties of magnetic fluids on particle size. *J Magn Magn Mater*. 1995;149:72–78.
137. Gilles G, Bonville P, Rakoto H, Broto JM, Wong KK, Mann S. Magnetic hysteresis and superantiferromagnetism in ferritin nanoparticles. *J Magn Magn Mater*. 2002;241:430–440.
138. Makhlof SA, Parker FT, Berkowitz AE. Magnetic hysteresis anomalies in ferritin. *Phys Rev B Condens Matter Mater Phys*. 1997;55: R14717–R14720.
139. Koralewski M, Pochylski M, Mitroova Z, Timko M, Kopcansky P, Melnikova L. Magnetic birefringence of natural and synthetic ferritin. *J Magn Magn Mater*. 2011;323:2413–2417.
140. Guertin RP, Harrison N, Zhou ZX, McCall S, Drymiotis F. Very high field magnetization and AC susceptibility of native horse spleen ferritin. *J Magn Magn Mater*. 2007;308:97–100.
141. Silva NJ, Millan A, Palacio F, et al. Temperature dependence of anti-ferromagnetic susceptibility of ferritins. *Phys Rev B Condens Matter*. 2009;79:104405.
142. Chuanlin L, Yunan H, Chenghua G, Chengsheng L, Xiguang C. Properties of biogenic magnetite nanoparticles in the radula of chiton *Acanthochiton rubrolineatus* Lischke. *J Wuhan Univ Technol Mater Sci*. 2011;26:478–482.
143. Papaefthymiou GC. The Mössbauer and magnetic properties of ferritin cores. *Biochim Biophys Acta*. 2010;1800:886–897.
144. Oshtrakh MI, Alenkina IV, Kuzmann E, Klencsar Z, Siemionkin VA. Anomalous Mössbauer line broadening for nanosized hydrous ferric oxide cores in ferritin and its pharmaceutical analogue Ferum Lek in the temperature range 295–90 K. *J Nanopart Res*. 2014; 16:2363.
145. Joos A, Rümenapp C, Wagner FE, Gleich B. Characterisation of iron oxide nanoparticles by Mössbauer spectroscopy at ambient temperature. *J Magn Magn Mater*. 2016;399:123–129.
146. Jin WY, Xu GZ, Scialabassi J, Zhu JG, Bagic A, Sun MG. Detection of magnetic nanoparticles with magnetoencephalography. *J Magn Magn Mater*. 2008;320:1472–1478.
147. Pan YH, Sader K, Powell JJ, et al. 3D morphology of the human hepatic ferritin mineral core: new evidence for a subunit structure revealed by single particle analysis of HAADF-STEM images. *J Struct Biol*. 2009; 166:22–31.
148. Quintana C, Lancin M, Marhic C, Pérez M, Avila J, Carrascosa JL. Preliminary high resolution TEM and electron energy loss spectroscopy studies of ferritin cores extracted from brain in patients with neurodegenerative PSP and Alzheimer diseases. *Cell Mol Biol*. 2000;46:807–820.

149. Gossuin Y, Hautot D, Muller RN, et al. Looking for biogenic magnetite in brain ferritin using NMR relaxometry. *NMR Biomed*. 2005; 18:469–472.
150. Passeri D, Dong C, Reggente M, et al. Magnetic force microscopy: quantitative issues in biomaterials. *Biomater*. 2014;4:e29507.
151. Daniels SL, Ngunjiri JN, Garno JC. Investigation of the magnetic properties of ferritin by AFM imaging with magnetic sample modulation. *Anal Bioanal Chem*. 2009;394:215–223.
152. Mikhaylova A, Davidson M, Toastmann H, et al. Detection, identification and mapping of iron anomalies in brain tissue using X-ray absorption spectroscopy. *J R Soc Interface*. 2005;2:33–37.
153. Espinosa A, Serrano A, Llavona A, et al. On the discrimination between magnetite and maghemite by XANES measurements in fluorescence mode. *Meas Sci Technol*. 2012;23:015602.
154. Gálvez N, Fernández B, Sánchez P, et al. Comparative structural and chemical studies of ferritin cores with gradual removal of their iron contents. *J Am Chem Soc*. 2008;130:8062–8068.
155. Melniková L, Petrenko VI, Avdeev MV, et al. Effect of iron oxide loading on magnetoferritin structure in solution as revealed by SAXS and SANS. *Colloids Surf B Biointerfaces*. 2014;123:82–88.
156. Pershant PS. Magneto-optical effects. *J Appl Phys*. 1967;38: 1482–1490.
157. Koralewski M, Pochylski M, Gierszewski J. Magnetic birefringence of iron oxyhydroxide nanoparticles stabilised by sucrose. *J Magn Magn Mater*. 2011;323:1140–1144.
158. Koralewski M, Pochylski M, Mitróová Z, et al. Magnetic birefringence study of the magnetic core structure of ferritin. *Acta Phys Pol A*. 2012;121:1237–1239.
159. Koralewski M, Klos JW, Baranowski M, et al. The Faraday effect of natural and artificial ferritins. *Nanotechnology*. 2012;23:355704.
160. Koralewski M, Pochylski M, Gierszewski J. Magnetic properties of ferritin and akaganeite nanoparticles in aqueous suspension. *J Nanopart Res*. 2013;15:1902.
161. Dobosz B, Krzyminewski R, Koralewski M, Hałupka-Bryl M. Computer enhancement of ESR spectra of magnetite nanoparticles. *J Magn Magn Mater*. 2016;407:114–121.
162. Wajnberg E, El-Jaick LJ, Linhares MP, Esquivel DM. Ferromagnetic resonance of horse spleen ferritin: core blocking and surface ordering temperatures. *J Magn Reson*. 2001;153:69–74.
163. Newman DM, Heptinstall J, Matelon RJ, et al. A magneto-optic route toward the in vivo diagnosis of malaria: preliminary results and preclinical trial data. *Biophys J*. 2008;95:994–1000.
164. Mens PF, Matelon RJ, Nour BY, Newman DM, Schallig HD. Laboratory evaluation on the sensitivity and specificity of a novel and rapid detection method for malaria diagnosis based on magneto-optical technology (MOT). *Malaria J*. 2010;9:207.
165. Ku BY, Chan ML, Ma Z, Horsley DA. Frequency-domain birefringence measurement of biological binding to magnetic nanoparticles. *J Magn Magn Mater*. 2008;320:2279–2283.
166. Wang W, Knovich MA, Coffman LG, Torti FM, Torti SV. Serum ferritin: past, present and future. *Biochim Biophys Acta*. 2010;1800: 760–769.
167. Worwood M. Ferritin. *Blood Rev*. 1990;4:259–269.
168. Cozzi A, Rovelli E, Frizzale G, et al. Oxidative stress and cell death in cells expressing L-ferritin variants causing neuroferritinopathy. *Neurobiol Dis*. 2009;37:77–85.
169. Galazka-Friedman J, Bauminger ER, Szlachta K, Friedman A. The role of iron in neurodegeneration: Mössbauer spectroscopy, electron microscopy, enzyme-linked immunosorbent assay and neuroimaging studies. *J Phys Condens Matter*. 2012;24:244106.
170. Hautot D, Pankhurst QA, Morris CM, Curtis A, Burn J, Dobson J. Preliminary observation of elevated levels of nanocrystalline iron oxides in the basal ganglia of neuroferritinopathy patients. *Biochim Biophys Acta*. 2007;1772:21–25.
171. Céspedes O, Ueno S. Effect of radio frequency magnetic fields on iron release from cage proteins. *Bioelectromagnetics*. 2009;30: 336–342.
172. Céspedes O, Inamoto O, Kai S, Nibu Y, et al. Radio frequency magnetic fields effects on molecular dynamics and iron uptake in cage proteins. *Bioelectromagnetics*. 2010;31:311–317.
173. Webb J, Macey DJ, Chua-Ansuom W, et al. Iron biominerals in medicine and the environment. *Coord Chem Rev*. 1999;190–192:1199–1215.
174. Allen PD, St Pierre TG, Chua-Ansuom W, Ström V, Rao KV. Low-frequency low-field magnetic susceptibility of ferritin and hemosiderin. *Biochim Biophys Acta*. 2000;1500:186–196.
175. Miyazaki E, Kato J, Kobune M, et al. Denaturated H-ferritin is a major constituent of hemosiderin in the liver of patient with iron overload. *Gut*. 2002;50:413–419.
176. Williams JM, Andrews SC, Treffry A, Harrison PM. The relationship between ferritin and haemosiderin. *Hyperfine Interact*. 1986;29: 1447–1450.
177. Webb J, St Pierre TG, Tran KC, Chua-Anusom W, Macey DJ, Pootrakul P. Biologically significant iron(III) oxyhydroxy polymers: Mössbauer spectroscopic study of ferritin and hemosiderin in pancreas tissue of  $\beta$ -thalassaemia/hemoglobin E disease. *Inorg Chim Acta*. 1996;243:121–125.
178. Cai Y, Cao Ch, He X, et al. Enhanced magnetic resonance imaging and staining of cancer cells using ferromagnetic H-ferritin nanoparticles with increasing core size. *Int J Nanomedicine*. 2015;10: 2619–2634.
179. Schwartz J, Liu XS, Tosa T, Thiel EC, Solomon EI. Spectroscopic definition of the ferroxidase site in M ferritin: comparison of binuclear substrate vs cofactor active sites. *J Am Chem Soc*. 2008;130: 9441–9450.
180. Meldrum FC, Heywood BR, Mann S. Magnetoferritin: in vitro synthesis of a novel magnetic protein. *Science*. 1992;257:522–523.
181. Klem MT, Young M, Douglas T. Biomimetic magnetic nanoparticles. *Mater Today*. 2005;8:28–37.
182. Uchida M, Kang S, Reichhardt C, Harlen K, Douglas T. The ferritin superfamily: supramolecular templates for materials synthesis. *Biochim Biophys Acta*. 2010;1800:834–845.
183. Valero E, Tambalo S, Marzola P, et al. Magnetic nanoparticles-templated assembly of protein subunits: new platforms for carbohydrate-based MRI nanoprobe. *J Am Chem Soc*. 2011;133:4889–4895.
184. Jutz G, Boeker A. Bionanoparticles as functional macromolecular building blocks: a new class of nanomaterial. *Polymer*. 2011;52:211–232.
185. Jääskeläinen A, Soukka T, Lammimäki U, Korpimäki T, Virta M. Development of a denaturation/renaturation-based production process for ferritin nanoparticles. *Biotechnol Bioeng*. 2009;102:1012–1024.
186. Yamashita I, Iwahori K, Kumaga S. Ferritin in the field on nanodevices. *Biochim Biophys Acta*. 2010;1800:846–857.
187. Crompton DE, Chinnery PF, Bates D, et al. Spectrum of movement disorders in neuroferritinopathy. *Mov Disord*. 2005;20:95–99.
188. Collingwood JF, Davidson MR. The role of iron in neurodegenerative disorders: insights and opportunities with synchrotron light. *Front Pharmacol*. 2014;5:191.
189. Everett J, Céspedes E, Shelford LR, et al. Ferrous iron formation following the co-aggregation of ferric iron and the Alzheimer's disease peptide  $\beta$ -amyloid (1–42). *J R Soc Interface*. 2014;11:20140165.
190. Hautot D, Pankhurst QA, Dobson J. Superconducting quantum interference device measurements of dilute magnetic materials in biological samples. *Rev Sci Instrum*. 2005;76:045101.
191. Dobson J. Nanoscale biogenic iron oxides and neurodegenerative disease. *FEBS Lett*. 2001;496:1–5.
192. Dobson J. Magnetic iron compounds in neurological disorders. *Ann N Y Acad Sci*. 2004;1012:183–192.
193. Pann Y, Brown YA, Brydson R, Warley A, Li A, Powell J. Electron beam damage studies of synthetic 6-line ferrihydrite and ferritin molecule cores within a human liver biopsy. *Micron*. 2006;37:403–411.
194. Koralewski M, Melniková L, Mitróová Z, Pochylski M, Baranowski M, Kopčanský P. Magneto-optical investigation of ferritin iron uptake and release. Poster presented at: 10th International Conference on the Scientific and Clinical Applications of Magnetic Carriers; June 10–14, 2014; Dresden, Germany.



195. Bilgic B, Pfefferbaum A, Rohlfing T, Sullivan EV, Adalsteinsson E. MRI estimates of brain iron concentration in normal aging using quantitative susceptibility mapping. *Neuroimage*. 2012;59:2625–2635.
196. Haacke EM, Cheng NY, House MJ, et al. Imaging iron stores in the brain using magnetic imaging. *Magn Reson Imaging*. 2005;23:1–25.
197. Langkammer C, Schweser F, Krebs N, et al. Quantitative susceptibility mapping (QSM) as a means to measure brain iron? A post mortem validation study. *Neuroimage*. 2012;62:1593–1599.
198. Langkammer C, Ropele S, Pirpamer L, Fazekas F, Schmidt R. MRI for iron mapping in Alzheimer's disease. *Neurodegener Dis*. 2014;13:189–191.
199. Ramos P, Santos A, Pinto NR, Mendes R, Magalhães T, Almeida A. Iron levels in the human brain: a post-mortem study of anatomical region differences age-related changes. *J Trace Elem Med Biol*. 2014;28:13–17.
200. Schweser F, Deistung A, Lehr BW, Reichenbach JR. Quantitative imaging of intrinsic magnetic tissue properties using MRI signal phase: an approach to in vivo brain iron metabolism? *Neuroimage*. 2011;54:2789–2807.
201. Miglierini M, Boca R, Kopáni M, Lancok A. Mössbauer and SQUID characterization of iron in human tissue: case of globus pallidus. *Acta Phys Pol A*. 2014;126:240–241.
202. Szybowicz M, Koralewski M, Karoń J, Melnikowa L. Micro-Raman spectroscopy of natural and synthetic ferritins and their mimetics. *Acta Phys Pol A*. 2015;127:534–536.
203. Stöckel S, Kirchhoff J, Neugebauer U, Rösch P, Popp J. The application of Raman spectroscopy for the detection and identification of microorganisms. *J Raman Spectrosc*. 2016;47:89–109.
204. Butler HJ, Ashton L, Bird B, et al. Using Raman spectroscopy to characterize biological materials. *Nat Protoc*. 2016;11:664–687.
205. Dunn JR, Fuller M, Zoeger J, et al. Magnetic material in the human hippocampus. *Brain Res Bull*. 1995;36:149–153.
206. Collingwood JF, Adams F. Chemical imaging analysis of the brain with X-ray methods. *Spectrochim Acta Part B*. 2017;130:101–118.
207. Dobson J, Grassi P. Magnetic properties of human hippocampal tissue: evaluation of artefact and contamination sources. *Brain Res Bull*. 1996;39:255–259.
208. Prozorov T, Mallapragada SK, Narasimhan B, et al. Protein-mediated synthesis of uniform superparamagnetic magnetite nanocrystals. *Adv Funct Mater*. 2007;17:951–957.
209. Amemiya Y, Arakaki A, Staniland SS, Tanaka T, Matsunaga T. Controlled formation of magnetite crystal by partial oxidation of ferrous hydroxide in the presence of recombinant magnetotactic. *Biomaterials*. 2007;28:5381–5389.
210. Arakaki A, Masuda F, Amemiya Y, Tanaka T, Matsunaga T. Control of the morphology and size of magnetite particles with peptides mimicking the Mms6 protein from magnetotactic bacteria. *J Colloid Interface Sci*. 2010;343:65–70.
211. Galloway JM, Arakaki A, Masuda F, Tanaka T, Matsunaga T, Staniland SS. Magnetic bacterial protein Mms6 controls morphology, crystallinity and magnetism of cobalt-doped magnetite nanoparticles in vitro. *J Mater Chem*. 2011;21:15244–15254.
212. Siponen MI, Legrand B, Widdrat M, et al. Structural insight into magnetochrome-mediated magnetite biomineralization. *Nature*. 2013;502:681–684.
213. Gorobets S, Gorobets O. Functions of biogenic magnetic nanoparticles in organisms. *Funct Mater*. 2012;19:18–26.
214. Gorobets S, Gorobets O, Demyanenko I. Ferritin and biomineralization of magnetic nanoparticles in microorganisms. *Res Bull NTUU*. 2013;3:34–41.
215. Matsunaga T, Okamura Y, Fukuda Y, Wahyudi AT, Murase Y, Takeyama H. Complete genome sequence of the facultative anaerobic magnetotactic bacterium *Magnetospirillum* sp. strain AMB-1. *DNA Res*. 2005;12:157–166.
216. Nakazawa H, Arakaki A, Narita-Yamada, et al. Whole genome sequence of *Desulfovibrio magneticus* strain RS-1 revealed common gene clusters in magnetotactic bacteria. *Genome Res*. 2009;19:1801–1808.
217. Methe BA, Nelson KE, Eisen JA, et al. Genome of *Geobacter sulfurreducens*: metal reduction in subsurface environments. *Science*. 2003;302:1967–1969.
218. Aklujkar M, Krushka J, DiBartolo G, Lapidus A, Land ML, Lovley DR. The genome sequence of *Geobacter metallireducens*: features of metabolism, physiology and regulation common and dissimilar to *Geobacter sulfurreducens*. *BMC Microbiol*. 2009;9:109–122.
219. Guo FF, Yang W, Jiang W, Geng S, Peng T, Li JL. Magnetosomes eliminate intracellular reactive oxygen species in *Magnetospirillum gryphiswaldense* MSR-1. *Environ Microbiol*. 2012;14:1722–1729.
220. Bush A. Copper, zinc, and the metallobiology of Alzheimer disease. *Alzheimer Dis Assoc Disord*. 2003;17:147–150.
221. House E, Esiri M, Forster G, Ince PG, Exley C. Aluminium, iron and copper in human brain tissues donated to the Medical Research Council's Cognitive Function and Ageing study. *Metallomics*. 2012;4:56–65.
222. Sidhu PS, Gilkes RJ, Posner AM. The synthesis and some properties of Co, Ni, Zn, Cu, Mn and Cd substituted magnetites. *J Inorg Nucl Chem*. 1978;40:429–435.
223. Tosha T, Ng HL, Bhattasali O, Alber T, Theil EC. Moving metal ions through ferritin-protein nanocages from three-fold pores to catalytic sites. *J Am Chem Soc*. 2010;132:14562–14569.
224. Iwahori K, Yamashita I. Size-controlled one-pot synthesis of fluorescent cadmium sulfide semiconductor nanoparticle in an apoferritin cavity. *Nanotechnology*. 2008;19:495601.
225. Kozłowski H, Luczkowski M, Remelli M, Valensin D. Copper, zinc and iron in neurodegenerative diseases (Alzheimer's, Parkinson's and prion diseases). *Coord Chem Rev*. 2012;256:2129–2141.
226. Wang X, Liang L. Effects of static magnetic field on magnetosome formation and expression of mamA, mms13, mms6 and magA in *Magnetospirillum magneticum* AMB-1. *Bioelectromagnetics*. 2009;4:313–321.
227. Wang X, Liang L, Song T, Wu L. Magnetosome formation and expression of mamA, mms13, mms6 and magA in *Magnetospirillum magneticum* AMB-1 exposed to pulsed magnetic field. *Curr Microbiol*. 2009;59:221–226.
228. Sonnier H, Marino AA. Sensory transduction as a proposed model for biological detection of electromagnetic fields. *Electro Magnetobiol*. 2001;20:153–175.
229. Jandacka P, Burda H, Pistora J. Magnetically induced behaviour of ferritin corpuscles in avian ears: can cuticulosomes function as magnetosomes? *J R Soc Interface*. 2015;12:20141087.
230. Gorobets Y, Gorobets S. Stationary flows of electrolytes in the vicinity of ferromagnetic particles in a constant magnetic field. *Bull Kherson State Tech Univ*. 2000;3:276–281.
231. Gorobets O. Biomagnetism and biogenic magnetic nanoparticles. *Her Natl Acad Sci Ukr*. 2015;7:53–64.
232. Banachlocha MA, Bókkon I, Banachlocha HM. Long-term memory in brain magnetite. *Med Hypotheses*. 2010;74:254–257.
233. Bókkon I, Salari V. Information storing by biomagnetites. *J Biol Phys*. 2010;36:109–120.
234. Hand E. Joe Kirschvink thinks he has found a magnetic sixth sense in humans. *Science*. 2016;352:1509–1513.



**International Journal of Nanomedicine****Dovepress****Publish your work in this journal**

The International Journal of Nanomedicine is an international, peer-reviewed journal focusing on the application of nanotechnology in diagnostics, therapeutics, and drug delivery systems throughout the biomedical field. This journal is indexed on PubMed Central, MedLine, CAS, SciSearch®, Current Contents®/Clinical Medicine,

Journal Citation Reports/Science Edition, EMBase, Scopus and the Elsevier Bibliographic databases. The manuscript management system is completely online and includes a very quick and fair peer-review system, which is all easy to use. Visit <http://www.dovepress.com/testimonials.php> to read real quotes from published authors.

Submit your manuscript here: <http://www.dovepress.com/international-journal-of-nanomedicine-journal>